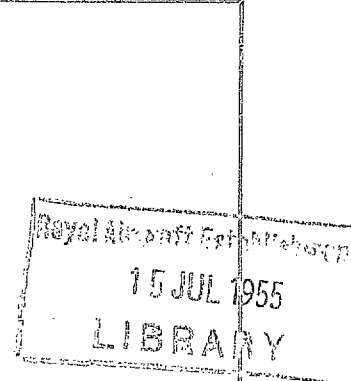
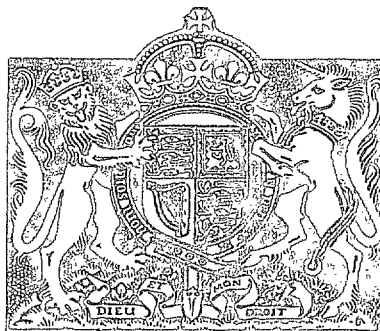


N.A.E.

R. & M. No. 2683  
(10,933)  
A.R.C. Technical Report



MINISTRY OF SUPPLY

AERONAUTICAL RESEARCH COUNCIL  
REPORTS AND MEMORANDA

# The Application of the Exact Method of Aerofoil Design

By

M. B. GLAUERT, M.A.,

of the Aerodynamics Division, N.P.L.

*Crown Copyright Reserved*

LONDON : HER MAJESTY'S STATIONERY OFFICE

1955

TWELVE SHILLINGS NET

# The Application of the Exact Method of Aerofoil Design

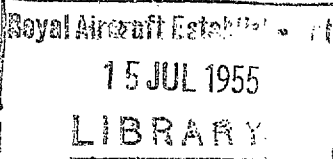
By

M. B. GLAUERT, M.A.,

of the Aerodynamics Division, N.P.L.

*Reports and Memoranda No. 2683\**

*October, 1947*



*Summary.*—This report considers in detail the design of aerofoils by Lighthill's exact method, in which the velocity over the aerofoil surface is prescribed as a function of the angular co-ordinate on the circle into which the aerofoil may be transformed. The mathematical basis of the method is set out, means for obtaining desired characteristics for the aerofoil are developed, and the procedure to be followed in the actual design is fully discussed. Various special functions are introduced to increase the range and practical utility of the velocity distributions obtainable, and these and other functions are fully tabulated. The calculations for the design of a particular thick suction aerofoil are set out in detail.

1. *Introduction.*—Lighthill has presented in R. & M. 2112<sup>1</sup> a new method for the design of aerofoils. It enables the velocity distribution over the aerofoil surface in two-dimensional incompressible flow to be prescribed arbitrarily, provided certain integral relations are satisfied. The velocity is taken as a function of the angular co-ordinate  $\theta$  on the circle to which the aerofoil corresponds, in the conformal transformation between the region outside the aerofoil and the region outside the circle. It is shown that the logarithm of the velocity, and the direction of flow on the aerofoil surface, are Fourier conjugate functions of  $\theta$ . This enables the aerofoil shape to be calculated. The method is exact, in that there are no approximations or restrictions as to lift coefficient, thickness, or camber, but numerical integration is necessary to obtain the co-ordinates of the aerofoil surface.

A full exposition of the method is given in R. & M. 2112<sup>1</sup>, and a large number of examples are worked out. The present report extends the analysis slightly in certain directions, but its main purpose is to develop special terms which may be incorporated in the velocity distribution to produce certain desired characteristics, and to provide a list of the Fourier conjugates and various associated integrals of functions which are in general use. The practical procedure recommended for the design of an aerofoil is also fully discussed.

The principal feature of Lighthill's method is that it does not attempt to determine completely the relationship between the aerofoil and circle planes ; it merely seeks to establish enough about it to enable the aerofoil shape to be calculated, and the aerodynamic characteristics of the aerofoil to be found. The method is very flexible and can produce aerofoils of widely varying types. It affords the only satisfactory means of designing suction aerofoils, which are required to have discontinuities in the velocity over the surface. If the velocity distribution chosen is of a simple nature, the calculations can be carried through very speedily, with the aid of a calculating machine, but the work involved increases rapidly as the selected distribution

\* Published with the permission of the Director, National Physical Laboratory.

becomes more complicated. Only functions simple enough for their conjugates to be evaluable can be used in prescribing the velocity. As a result the number of disposable parameters is limited, and for thin aerofoils of conventional form, approximate methods probably give superior results, unless an exact velocity distribution is particularly desired. The method cannot be used to find the velocity over a given aerofoil, nor can it estimate the effects of modifications to a designed profile.

The method has numerous further applications. Lighthill employed it in R. & M. 2112<sup>1</sup> to design two-dimensional contractions and aerofoils in cascade, and it may also be used to obtain bends for wind tunnels and to design the suction slot at the same time as the rest of a suction aerofoil. These and other fresh developments lie outside the scope of the present report.

2. *The Mathematical Method.*—For the steady irrotational two-dimensional flow of an incompressible inviscid fluid, there exists a complex potential  $w = \phi + i\psi$  which is an analytic function  $w(z)$  of the complex variable of position  $z = x + iy$ .  $\phi$  is the velocity potential and  $\psi$  the stream function.

It follows that

where  $q$  is the magnitude of the fluid velocity and  $\chi$  the direction the flow makes with the  $x$ -axis.  $u$  and  $v$  are the velocity components in the direction of the axes.

Now if a conformal transformation of the region of flow in the  $z$ -plane is made to another region in the  $\zeta$ -plane, by means of the transformation function  $z = g(\zeta)$ , then  $w = w\{g(\zeta)\}$  gives the flow in the  $\zeta$ -plane, with boundary conditions to be found from the transformation.

The flow in the  $\zeta$ -plane round the unit circle  $|\zeta| = 1$ , with the velocity at infinity unity at an angle  $\alpha$  with the real axis, is given by

$$w = \zeta e^{-ia} + \frac{1}{\zeta e^{-ia}} + i\pi \log \zeta, \quad \dots \quad \dots \quad \dots \quad \dots \quad \dots \quad (2)$$

where  $2\pi\nu$  is the circulation round the circle,

$$\frac{dw}{d\xi} = \frac{1}{\xi} \left\{ \zeta e^{-ia} - \frac{1}{\zeta e^{-ia}} + ia \right\}. \quad \dots \quad \dots \quad \dots \quad \dots \quad \dots \quad (3)$$

On the circle itself  $\zeta = e^{i\theta}$ , and here

$$\frac{dw}{d\xi} = i e^{-i\theta} \{ 2 \sin(\theta - \alpha) + \kappa \} . \quad \dots \quad \dots \quad \dots \quad \dots \quad \dots \quad (4)$$

Thus the velocity over the surface of the circle

$$= \left| \frac{d\omega}{d\xi} \right| = |2 \sin(\theta - \alpha) + \varkappa|. \quad \dots \quad \dots \quad \dots \quad \dots \quad \dots \quad (5)$$

For  $\alpha = 0$ , this shows there are stagnation points on the circle at  $\theta = \alpha$  and  $\theta = \pi + \alpha$ , as would be expected.

Suppose now the region outside the circle is conformally transformed into the region outside an aerofoil, in the  $z$ -plane, by means of an analytic function  $z(\xi)$ , such that a definite point on the aerofoil, the trailing edge, corresponds to the point  $\xi = 1$  on the circle. Also let  $z - \xi \rightarrow 0$  as  $\xi \rightarrow \infty$ . This ensures that the conditions at infinity are the same in the two planes.

By the Kutta-Joukowsky condition the velocity must be zero on the circle at  $\theta = 0$ , the point corresponding to the trailing edge. Hence by equation (5)

$$z = 2 \sin \alpha, \quad \dots \quad (6)$$

and

$$\left| \frac{dw}{d\zeta} \right| = \left| 4 \sin \frac{\theta}{2} \cos \left( \frac{\theta}{2} - \alpha \right) \right|. \quad \dots \quad \dots \quad \dots \quad \dots \quad \dots \quad (7)$$

In the aerofoil plane let  $dw/dz = q e^{-iz}$ . On the aerofoil itself  $q$  is the surface velocity and  $\chi$  is the direction of the tangent.

Then

$$q = \left| \frac{dw}{dz} \right| = \frac{dw}{d\xi} \cdot \frac{d\xi}{dz} .$$

On the aerofoil surface  $dz = ds \cdot e^{ix}$ , where  $s$  is the distance along the surface. Hence on the aerofoil at incidence  $\alpha$ , ignoring for the present the question of sign, from equation (7)

$$q_a = 4 \sin \frac{\theta}{2} \cos \left( \frac{\theta}{2} - \alpha \right) \cdot \frac{d\theta}{ds}, \quad \dots \quad \dots \quad \dots \quad (8)$$

Now  $dx = ds \cos \chi$ ,  $dy = ds \sin \chi$ , hence

$$\left. \begin{aligned} x &= \int \frac{2 \sin \theta}{q_0} \cos \chi \, d\theta, \\ y &= \int \frac{2 \sin \theta}{q_0} \sin \chi \, d\theta. \end{aligned} \right\} \dots \quad \dots \quad \dots \quad \dots \quad \dots \quad \dots \quad (11)$$

Consequently if  $q_0$  is prescribed as a function of the circle co-ordinate  $\theta$ , the aerofoil contour can at once be found if  $\chi$  is known.

Further from equations (8) and (9)

$$q_\alpha = q_0 \frac{\cos\left(\frac{\theta}{2} - \alpha\right)}{\cos\frac{\theta}{2}} \quad \dots \quad \dots \quad \dots \quad \dots \quad \dots \quad \dots \quad (12)$$

so a knowledge of  $q_0$  implies a knowledge of  $q$  at any other incidence.

Now since  $z - \xi \rightarrow 0$  as  $\xi \rightarrow \infty$ , we may write

Hence

$$\frac{dz}{d\xi} = 1 - \frac{a_1}{\xi^2} - \dots \dots \dots \dots \dots \dots \dots \quad (14)$$

Also

$$\frac{d\omega_0}{d\xi} = 1 - \frac{1}{\xi^2}, \text{ from equation (3),} \quad \dots \quad \dots \quad \dots \quad \dots \quad (15)$$

and so

$$\frac{dw_0}{dz} = \frac{dw_0}{d\xi} \cdot \frac{d\xi}{dz} = 1 - \frac{1 + a_1}{\xi^2} - \dots \dots \dots \dots \dots \dots \dots \quad (16)$$

and

$$\log \frac{dw_0}{dz} = -\frac{1+a_1}{\zeta^2} - \dots$$

$= \sum_{n=2}^{\infty} \frac{b_n + ic_n}{\zeta^n}$ , say, where  $b_n$  and  $c_n$  are real. .. .. (17)

Now

$$\frac{d\omega_0}{dz} = q_0 e^{-iz}$$

hence

Thus on the circle  $\zeta = e^{i\theta}$ , from equation (17),

$$\log q_0 - i\chi = \sum_{n=1}^{\infty} (b_n + i c_n) (\cos n\theta - i \sin n\theta).$$

Equating real and imaginary parts

$$\left. \begin{aligned} \log q_0 &= \sum_{n=2}^{\infty} (b_n \cos n\theta + c_n \sin n\theta) \\ \chi &= \sum_{n=2}^{\infty} (b_n \sin n\theta - c_n \cos n\theta) \end{aligned} \right\} \quad \dots \quad \dots \quad \dots \quad \dots \quad (19)$$

which are conjugate Fourier series.

Hence  $\log q_0$  and  $\chi$  are conjugate functions of  $\theta$ . Poisson's integral relating conjugate functions is

$$\chi(\theta) = \frac{1}{2\pi} \int_{-\pi}^{\pi} \log q_0(t) \cot \frac{1}{2}(\theta - t) dt \quad \dots \quad \dots \quad \dots \quad \dots \quad (20)$$

where the Cauchy principal value must be taken at the singularity  $t = 0$ .

If  $\log q_0$  is an even function of  $\theta$ , as in a symmetrical aerofoil,  $\chi$  is an odd function and equation (20) simplifies to

$$\chi(\theta) = -\frac{\sin \theta}{\pi} \int_0^\pi \frac{\log q_0(t)}{\cos \theta - \cos t} dt, \quad \dots \quad \dots \quad \dots \quad \dots \quad (21)$$

and if  $\log q_0$  is an odd function of  $\theta$ ,

$$\chi(\theta) = -\frac{1}{\pi} \int_0^\pi \frac{\log q_0(t) \sin t}{\cos \theta - \cos t} dt, \quad \dots \quad \dots \quad \dots \quad \dots \quad (22)$$

in each case the Cauchy principal value being taken.

It is seen from equation (19) that the Fourier series for  $\log q_0$  contains terms only with  $n \geq 2$ . It follows that

$$\left. \begin{array}{l} A. \quad \int_{-\pi}^{\pi} \log q_0 d\theta = 0 \\ B. \quad \int_{-\pi}^{\pi} \log q_0 \cos \theta d\theta = 0 \\ C. \quad \int_{-\pi}^{\pi} \log q_0 \sin \theta d\theta = 0 \end{array} \right\} \quad \dots \quad \dots \quad \dots \quad \dots \quad (23)$$

Physically, the first of these equations says that the velocity at infinity must be unity, and the remaining two require that the aerofoil contour shall close up.

The design method is now clear.  $\log q_0$  is prescribed over the aerofoil as a function of  $\theta$ , with three arbitrary parameters whose values are determined by equation (23).  $\chi$  is then found as the conjugate function, and the aerofoil shape is calculated from equation (11) by numerical integration. The art is to choose a distribution of  $\log q_0$  which enables the design requirements to be satisfied, and is simple enough to allow the integral for  $\chi$  to be evaluated and the aerofoil shape to be computed, without undue labour.

When the shape has been calculated the chord is found, and its length is measured. This turns out to be a quantity  $c$  rather less than 4. Now the aerodynamic characteristics of the aerofoil can be determined.

From equation (6) the circulation is  $4\pi \sin \alpha$ ,

hence  $C_L = \frac{8\pi}{c} \sin \alpha. \quad \dots \quad \dots \quad \dots \quad \dots \quad \dots \quad (24)$

The lift-curve slope is  $8\pi/c$ , and so is rather greater than  $2\pi$ .

For the pitching moment, by Blasius' theorem, the nose-up moment at zero lift is the real part of

$$M = \frac{1}{2} \rho_0 \int \left( \frac{dw_0}{dz} \right)^2 z dz. \quad \dots \quad \dots \quad \dots \quad \dots \quad \dots \quad (25)$$

By equation (17),

$$\frac{d\omega_0}{dz} = 1 + \frac{b_2 + ic_2}{\xi^2} + \dots, \\ = 1 + \frac{b_2 + ic_2}{z^2} + \dots, \quad \dots \quad \dots \quad \dots \quad \dots \quad \dots \quad (26)$$

since  $z - \xi \rightarrow 0$  as  $\xi \rightarrow \infty$ .

Hence

$$M = \frac{1}{2}\rho \cdot 2\pi i \cdot 2(b_2 + ic_2) \cdot \dots \cdot \dots \cdot \dots \quad (27)$$

The nose-up moment is therefore  $-2\pi\rho c_2$ .

But from equation (19),  $c_2 = \frac{1}{\pi} \int_{-\pi}^{\pi} \log q_0 \sin 2\theta \, d\theta$ , and hence

$$C_{M0} = -\frac{4}{G^2} \int_{-\pi}^{\pi} \log q_0 \sin 2\theta \, d\theta. \quad \dots \quad \dots \quad \dots \quad \dots \quad (28)$$

For the pitching moment at other incidences, see R. & M. 2112<sup>1</sup>. It is there shown that the aerodynamic centre is at a distance

$$\frac{1}{c} \left( 1 + \frac{1}{\pi} \int_{-\pi}^{\pi} \log q_0 \cos 2\theta \, d\theta \right) \text{ aerofoil chords forward of } z = 0. \quad \dots \quad (29)$$

Since

$$z - \zeta \rightarrow 0 \text{ as } \zeta \rightarrow \infty$$

$$z - \zeta = \sum_{n=1}^{\infty} \frac{a_n}{\zeta^n},$$

which becomes

$$z = \cos \theta - i \sin \theta = \sum_{n=1}^{\infty} a_n (\cos n\theta - i \sin n\theta), \quad \dots \quad \dots \quad (30)$$

on the circle where  $\zeta = e^{i\theta}$ . Thus  $z$  is a Fourier series in  $\theta$  with no constant term. Hence

This enables the position of  $z = 0$  on the aerofoil to be found, once the ordinates and abscissae have been obtained relative to arbitrary axes. The mean value with respect to  $\theta$  must be zero in each case. The position of the aerodynamic centre can then be calculated from equation (29).

If in computation no constants have been omitted from  $\chi$ , as they may be without affecting the resulting shape, the aerofoil as integrated is at the no-lift altitude. The incidence  $\alpha$  occurring in equation (24) must be measured from this position.

Thus practically all the aerodynamic characteristics of the aerofoil can be easily found. The evaluation of the velocity at points off the surface of the aerofoil is complicated, but a discussion of the problem is given in R. & M. 2112<sup>1</sup>.

*3. Design at Incidence.*—It is now time to turn to the problem of designing an actual aerofoil. The usual procedure is to employ the method of direct design at incidence, in which the upper surface velocity is prescribed at an incidence  $\alpha_1$ , and the lower surface velocity at a lower

incidence  $\alpha_2$ . The range of incidence from  $\alpha_2$  to  $\alpha_1$  is referred to as the incidence range of the aerofoil. It follows from equation (12), that on the upper surface

$$\log q_0 = \log \left| \frac{\cos \frac{\theta}{2}}{\cos \left( \frac{\theta}{2} - \alpha_1 \right)} \right| + \log q_{\alpha_1} . \quad \dots \quad \dots \quad \dots \quad (32)$$

and on the lower surface

$$\log q_0 = \log \left| \frac{\cos \frac{\theta}{2}}{\cos \left( \frac{\theta}{2} - \alpha_2 \right)} \right| + \log q_{\alpha_2} . \quad \dots \quad \dots \quad \dots$$

Where the upper and lower surfaces join,

$$\cos \left( \frac{\theta}{2} - \alpha_1 \right) = \pm \cos \left( \frac{\theta}{2} - \alpha_2 \right) ,$$

and so

$$\theta = \alpha_1 + \alpha_2 \text{ or } \theta = \pi + \alpha_1 + \alpha_2 . \quad \dots \quad \dots \quad \dots \quad \dots \quad (33)$$

The upper and lower surfaces join near the nose at  $\theta = \pi + \alpha_1 + \alpha_2$ . It is convenient to call this point the leading edge, though it may in fact not be the point farthest from the trailing edge.

Thus for a cambered aerofoil, the general expression taken for the velocity distribution is

$$\log q_0 = \left\{ \begin{array}{l} \log \left| \frac{\cos \frac{\theta}{2}}{\cos \left( \frac{\theta}{2} - \alpha_1 \right)} \right| , \quad \alpha_1 + \alpha_2 < \theta < \pi + \alpha_1 + \alpha_2 \\ + \log \left| \frac{\cos \frac{\theta}{2}}{\cos \left( \frac{\theta}{2} - \alpha_2 \right)} \right| , \quad \pi + \alpha_1 + \alpha_2 < \theta < 2\pi + \alpha_1 + \alpha_2 \\ + S \quad , \quad 0 < \theta < 2\pi \end{array} \right\} \quad \dots \quad (34)$$

$S$  is the value of  $\log q_{\alpha_1}$  on the upper surface, and of  $\log q_{\alpha_2}$  on the lower surface. If  $S$  is chosen as a simple function of  $\theta$  over the circle its conjugate can be determined. The conjugate of the first two terms of equation (34), and their contributions to the integrals of equation (23), are very important. These are calculated in Appendix II, and listed in Appendix I, both in the general case and in various special cases such as  $\alpha_2 = -\alpha_1$ , for a symmetrical aerofoil, and  $\alpha_2 = 0$ , for an aerofoil with the bottom of the incidence range at  $\alpha = 0$ . The conjugate is

$$F(T) = \frac{2}{\pi} \int_0^T \frac{\log x}{x^2 - 1} dx , \quad \dots \quad \dots \quad \dots \quad \dots \quad \dots \quad (35)$$

where  $T = \tan \frac{1}{2}(\theta - \alpha_1 - \alpha_2) \tan \frac{1}{2}(\alpha_1 - \alpha_2)$ . This integral has been evaluated numerically and is tabulated in Table 1.

At first sight it may appear difficult to prescribe a velocity distribution in terms of  $\theta$  to give an aerofoil with the required properties. Experience helps considerably. For a flat plate the transformation to a circle gives  $x = 2 \cos \theta$ , and in most aerofoils  $x$  varies rather like  $\cos \theta$ . The conjugates of a large number of functions suitable for use in  $S$  are listed in Appendix I, and also the corresponding expressions to be used in satisfying equation (23).

For a symmetrical aerofoil,  $\alpha_1 = -\alpha_2 = \alpha$ , say, and equation (34) takes the simpler form

$$\log q_0 = \log \left| \frac{\cos \frac{\theta}{2}}{\cos(\frac{\theta}{2} - \alpha)} \right| + S, \quad 0 < \theta < \pi \quad \dots \quad \dots \quad (36)$$

in which  $S = \log q_a$  and  $\log q_0$  is an even function of  $\theta$ .

As an example, a low-drag aerofoil may be considered, in which

$$S = \begin{cases} l & , \quad 0 < \theta < \pi \\ -k(\cos \theta - \cos \beta) & , \quad 0 < \theta < \beta \end{cases} \quad \dots \quad \dots \quad \dots \quad \dots \quad (37)$$

Here the velocity is constant at the design incidence back to  $\theta = \beta$ , and thereafter falls steadily. It is necessary to satisfy equation (23). Of the three equations, c holds automatically for a symmetrical aerofoil. The other two equations, taken over the range  $[0, \pi]$  only, can be written as follows, using Appendix I.

$$\left. \begin{array}{l} A. \quad l\pi - k(\sin \beta - \beta \cos \beta) - \pi\{X(\pi - 2\alpha) + X(2\alpha) - X(\pi)\} = 0 \\ B. \quad -\frac{1}{4}k\{2\beta - \sin 2\beta\} + k \cos \beta \sin \beta + \pi \sin^2 \alpha + \sin 2\alpha \log \cot \alpha = 0 \end{array} \right\} \quad \dots \quad \dots \quad (38)$$

Having chosen  $\alpha$  and  $\beta$  to give the required incidence range and position of maximum velocity these two equations are solved to determine  $l$  and  $k$ .  $X(\theta) = -\frac{1}{\pi} \int_0^\theta \log \sin \frac{1}{2}t dt$ , and occurs in many conjugates. It is tabulated in Table 2.

$\chi$  is now found from Appendix I as

$$F(\tan \alpha \tan \frac{1}{2}\theta) - \frac{k\beta}{\pi} \sin \theta + \frac{k}{\pi} (\cos \theta - \cos \beta) \log \left| \frac{\sin \frac{1}{2}(\theta + \beta)}{\sin \frac{1}{2}(\theta - \beta)} \right| \quad \dots \quad \dots \quad \dots \quad (39)$$

Finally the aerofoil shape is obtained from equation (11), the integrand being tabulated at intervals of  $\theta$  suitable for numerical integration. Several aerofoils are worked out in detail in R. & M. 2112<sup>1</sup>. One of them is shown in Fig. 1.

If the same technique is applied to a cambered aerofoil, using equation (34), the aerofoil has the same velocity on the upper surface at the top of the incidence range, as on the lower surface at the bottom. This is usually undesirable.

The method employed in R. & M. 2112<sup>1</sup> to overcome the difficulty involves approximations. A more satisfactory method is as follows. From equation (34), at  $\theta = \pi + \alpha_1 + \alpha_2$ , although there is continuity of  $\log q_0$ ,  $d(\log q_0)/d\theta$  has a discontinuity of amount

$$-\cot \frac{1}{2}(\alpha_1 - \alpha_2) = -\cot \alpha_0, \text{ say}, \quad \dots \quad \dots \quad \dots \quad \dots \quad \dots \quad (40)$$

where  $\alpha_0 = \frac{1}{2}(\alpha_1 - \alpha_2)$  and is equal to half the extent of the incidence range.

Now if  $S$  is taken to include terms

$$\left\{ \begin{array}{l} m \\ + (\pi + \alpha_1 + \alpha_2 - \theta) \cot \alpha_0, \end{array} \begin{array}{l} , \beta < \theta < \pi + \alpha_1 + \alpha_2 - \varepsilon \\ \pi + \alpha_1 + \alpha_2 - \varepsilon < \theta < \pi + \alpha_1 + \alpha_2, \end{array} \right\} \dots \quad (41)$$

there is continuity of  $\log q_0$  and  $d(\log q_0)/d\theta$  at  $\theta = \pi + \alpha_1 + \alpha_2$ , and also continuity of  $\log q_0$  at  $\theta = \pi + \alpha_1 + \alpha_2 - \varepsilon$ , provided that

$$m = \varepsilon \cot \alpha_0. \quad \dots \quad \dots \quad \dots \quad \dots \quad \dots \quad \dots \quad (42)$$

The effect of this technique is to increase  $\log q_0$  on the upper surface by an amount  $m$ . The upper surface velocity at incidence  $\alpha_1$  is constant up to  $\theta = \pi + \alpha_1 + \alpha_2 - \varepsilon$ . At incidence  $\alpha_2$ , the lower surface velocity rises very slowly between  $\theta = \pi + \alpha_1 + \alpha_2 - \varepsilon$  and  $\theta = \pi + \alpha_1 + \alpha_2$ , and from then on is constant. Effectively the leading edge has been moved to  $\theta = \pi + \alpha_1 + \alpha_2 - \varepsilon$ .

Complications arise in satisfying equation (23).  $m$  may conveniently be taken as one of the arbitrary parameters in  $\log q_0$ , but the equations are no longer linear. Since  $\cot \alpha_0$  is large,  $\varepsilon$  is small, and a method of successive approximations may be used. Without making use of equation (42), all the other parameters are eliminated from equation (23), leaving one equation connecting  $m$  and  $\varepsilon$ . With  $\varepsilon = 0$  this equation becomes linear in  $m$  and can at once be solved, giving  $m = m_1$ . Now from equation (42), write  $\varepsilon = m_1 \tan \alpha_0$  and a modified linear equation for  $m$  is obtained, yielding a second approximation  $m = m_2$ , and so on. The process converges very rapidly, three or four applications sufficing to calculate  $m$  to six decimal places. The remaining parameters can now be found as usual. In Appendix IV, an aerofoil is designed making use of this technique.

*4. The Leading Edge.*—It has been pointed out in the discussion of the  $\varepsilon$  technique, that when using the method of design at incidence, there is a discontinuity in  $d(\log q_0)/d\theta$  of amount  $-\cot \alpha_0$  at the leading edge. The  $\varepsilon$  term only shifts the discontinuity along the surface. Now if a function has a discontinuity, its conjugate function has a logarithmic infinity at the same point.

Thus the conjugate of  $k$ ,  $\lambda < \theta < \mu$  is  $\frac{k}{\pi} \log |[\sin \frac{1}{2}(\theta - \lambda)][\sin \frac{1}{2}(\theta - \mu)]|$ , which behaves like  $\frac{k}{\pi} \log(\theta - \lambda)$  near  $\theta = \lambda$ . The conjugate of  $d(\log q_0)/d\theta$  is  $d\chi/d\theta$ , as may be verified by differentiating the Fourier series (19), and hence  $d\chi/d\theta$  becomes logarithmically infinite at the leading edge. The curvature of the aerofoil surface  $= d\chi/ds = (dx/d\theta) \cdot (d\theta/ds)$ , so it also has a logarithmic infinity, since  $d\theta/ds$  remains finite and non-zero. If the discontinuity in  $d(\log q_0)/d\theta$  is small, the effect on the aerofoil shape is probably not serious; but  $\cot \alpha_0$  is large, particularly for fairly thin aerofoils. As a result of the zero radius of curvature, a high velocity peak will form at the nose at incidences above the top of the incidence range, limiting the maximum lift-coefficient of the aerofoil.

To avoid this, a term must be added to  $\log q_0$  to eliminate the discontinuity. Take a new co-ordinate  $\phi$  measured from the leading edge. Thus  $\phi = \theta - (\pi + \alpha_1 + \alpha_2 - \varepsilon)$ .

$$\text{Consider } K = \frac{1}{2n} \cot \alpha_0 \left\{ |n\phi| + \cos n\phi - \frac{\pi}{2} \right\}, \quad -\frac{\pi}{2n} < \phi < \frac{\pi}{2n}. \quad \dots \quad (43)$$

$$\text{At } \phi = 0, \quad \frac{dK}{d\phi} = \pm \frac{1}{2} \cot \alpha_0, \quad \dots \quad (44)$$

as required.

A full discussion is given in Appendix III, where it is shown that  $n = 3$  is sufficient to give a positive radius of curvature at the nose, provided the incidence range is at least 4 deg. Experience has shown that  $n = 6$  gives a better shaped nose and a reasonably large radius of curvature. If  $n$  is small there is a large reduction of velocity at  $\phi = 0$ , and the term extends over a wide range of  $\phi$ .

The conjugate function  $L_6$  and the Fourier constants are worked out in Appendix III. In Tables 3 and 4 the function  $L_6$  is tabulated in degrees, for both symmetrical and cambered aerofoils. For cambered aerofoils one of the terms of  $L_6$  cancels out with the term  $\cot \alpha_0 X(\phi)$  in the conjugate of the  $\varepsilon$  term, and so is not included. For symmetrical aerofoils the complete conjugate is tabulated directly in terms of  $\theta$ .

It may be noted that there is a second discontinuity of  $d(\log q_0)/d\theta$  at  $\theta = \alpha_1 + \alpha_2$ , of amount  $-\tan \alpha_0$ . This is small and can be safely ignored, since the aerofoil shape in this region near the trailing edge is not so important.

The leading-edge term  $K_6$  was used in the design of the aerofoil shown in Fig. 3. It will be seen that the nose is well rounded.

*5. The Trailing Edge.*—At the trailing edge the aerofoil shape is governed by the type of velocity distribution. With the normal choice of  $\log q_0$  in terms of simple trigonometrical functions of  $\theta$ , as for example in equation (37),  $\log q_0$  is finite at  $\theta = 0$ , and so  $q_0$  has a non-zero value there. As a result the trailing edge is cusped. A cusp gives good low-drag properties, and for most aerofoils no modification is required. When the cusped aerofoil has been designed, small modifications of shape may if necessary be made over the rear to thicken the trailing edge. The effect on the velocity distribution further forward is probably no greater than that produced in any case by the boundary layer over the tail.

If there is to be a finite trailing-edge angle  $\tau$ ,  $\chi$  must have a discontinuity  $-\tau$  at  $\theta = 0$ . Since  $\chi$  is the conjugate of  $\log q_0$ , near  $\theta = 0$

$$\log q_0 = \frac{\tau}{\pi} \log \theta + P, \quad \dots \quad \dots \quad \dots \quad \dots \quad \dots \quad \dots \quad (45)$$

where  $P$  is a function of  $\theta$ , finite at  $\theta = 0$ . Thus near  $\theta = 0$

$$q_0 = e^P \theta^{\tau/\pi}. \quad \dots \quad \dots \quad \dots \quad \dots \quad \dots \quad \dots \quad (46)$$

A suitable term to be included in  $\log q_0$  is

$$\frac{\tau}{\pi} \log \sin \theta, \quad -\frac{\pi}{2} < \theta < \frac{\pi}{2}, \quad \dots \quad \dots \quad \dots \quad \dots \quad \dots \quad (47)$$

whose conjugate is given in Appendix I. Experience has yet to be obtained as to the effect of various choices of  $P$  on the shape near the trailing edge.

When  $\tau = \pi$ , the trailing edge is rounded. The larger  $P$ , the smaller is the radius of curvature. Since this is usually required to be small,  $P$  should be chosen to rise rapidly as  $\theta$  decreases to 0. Probably a similar behaviour of  $P$  is also desirable when  $\tau$  is less than  $\pi$ .

In the normal case, when the aerofoil has a cusp, the usual choice of  $\log q$  gives similar velocities on the upper and lower surfaces near the trailing edge. It is sometimes necessary to produce

negative loading over the tail, by having a smaller velocity on the upper surface than on the lower.

If

$$\log q_0 = \begin{cases} 1 - \sin n\theta, & -\frac{\pi}{2n} < \theta < 0 \\ -1 - \sin n\theta, & 0 < \theta < \frac{\pi}{2n} \\ +S, & -\pi < \theta < \pi \end{cases} \dots \dots \dots \quad (48)$$

at the tail,  $S$  must be taken to be 2 greater on the lower surface than on the upper, to give continuity at  $\theta = 0$ . There are no discontinuities in either  $\log q_0$  or  $d(\log q_0)/d\theta$  at  $\theta = \pm \pi/2n$ . To spread the sharp change of velocity over a reasonable distance of the aerofoil surface,  $n$  is taken to be 6. The conjugate  $Q_6$  of the first two terms  $P_6$  of equation (48) is given in Appendix I, and tabulated in degrees in Table 5. It is employed in the design of the aerofoil considered in Appendix IV.

**6. Suction Aerofoils.**—The method of design is admirably suited to producing suction aerofoils. Several are worked out in R. & M. 2111<sup>4</sup> and 2112<sup>1</sup>. A distribution of  $\log q_0$  is chosen with a discontinuity  $k$  at some point  $\theta = \beta$ . The conjugate  $\chi$  contains a term  $-\frac{k}{\pi} \log |\sin \frac{1}{2}(\theta - \beta)|$ ,

and so has a logarithmic infinity at  $\theta = \beta$ . The shape of the surface near the discontinuity is shown in the next section to be approximately a logarithmic spiral, and methods are put forward for carrying out the integration in the neighbourhood to find the aerofoil co-ordinates. At this point on the surface, a suction slot is incorporated. Its primary purpose is to remove the boundary layer, which would otherwise separate owing to the sharp pressure rise, but there is also an effect on the velocity distribution, known as sink effect. The velocity is increased in front of the slot and decreased behind it.

For a sink of strength  $2\pi m$  on the circle at  $\theta = \beta$ , the complex potential of the flow round the circle becomes

$$w = \zeta e^{-ia} + \frac{1}{\zeta e^{-ia}} + iK \log \zeta - m \{2 \log (\zeta - e^{i\beta}) - \log \zeta\} \dots \dots \quad (49)$$

$$\frac{dw}{d\zeta} = e^{-ia} - \frac{1}{\zeta^2 e^{-ia}} + \frac{iK}{\zeta} - m \left\{ \frac{2}{\zeta - e^{i\beta}} - \frac{1}{\zeta} \right\} \dots \dots \dots \dots \quad (50)$$

Proceeding as before, the condition for a stagnation point at  $\theta = 0$  is

$$K = 2 \sin \alpha + m \cot \frac{\beta}{2} \dots \dots \dots \dots \dots \quad (51)$$

For a slot on the upper surface, suction produces an increase of circulation and hence of lift. The nearer the slot is to the trailing edge, the greater the gain. Using equation (51),

$$\left| \frac{dw}{d\zeta} \right| = \left| 4 \sin \frac{\theta}{2} \cos \left( \frac{\theta}{2} - \alpha \right) + m \cosec \frac{\beta}{2} \sin \frac{\theta}{2} \cosec \frac{\theta - \beta}{2} \right| \dots \dots \quad (52)$$

Hence if  $q_{am}$  is the velocity with suction at incidence  $\alpha$ ,

$$\frac{q_{am}}{q_0} = \left| \frac{\cos \left( \frac{\theta}{2} - \alpha \right)}{\cos \frac{\theta}{2}} + \frac{m}{4} \cosec \frac{\beta}{2} \cosec \frac{\theta - \beta}{2} \sec \frac{\theta}{2} \right|, \dots \dots \quad (53)$$

and

$$\frac{q_{am}}{q_a} = \left| 1 + \frac{m}{4} \operatorname{cosec} \frac{\beta}{2} \operatorname{cosec} \frac{\theta - \beta}{2} \sec \left( \frac{\theta}{2} - \alpha \right) \right|. \quad \dots \quad \dots \quad \dots \quad \dots \quad (54)$$

From these equations it is possible to calculate the modified potential velocity distribution.

The strength of the sink on the aerofoil is  $2\pi m/c$  where  $c$  is the number less than 4 occurring in equation (24). In the usual aerofoil notation, this sink strength is  $C_0 = Q/Uc$ , where  $Q$  is the volume sucked in unit time,  $U$  the stream velocity and  $c$  the aerofoil chord.

The effect of suction on the velocity distribution, as given by equation (54), is small except in the vicinity of the slot, but for an aerofoil with a slot at the nose this sink effect may be utilised to postpone the stall. In R. & M. 2162<sup>3</sup> the design of aerofoils to take advantage of this effect is considered.

It is also possible to design the aerofoil to take account of the suction directly. Suppose that at incidence  $\alpha$  with suction, there is a stagnation point behind the slot at  $\theta = \beta - \gamma$ . From equation (54),

$$m = 4 \cos \left( \frac{\beta - \gamma}{2} - \alpha \right) \sin \frac{\beta}{2} \sin \frac{\gamma}{2}, \quad \dots \quad \dots \quad \dots \quad \dots \quad (55)$$

then equation (53) becomes

$$\frac{q_{am}}{q_0} = \left| \frac{\sin \frac{1}{2}(\theta - \beta + \gamma) \cos \frac{1}{2}(\theta - \gamma - 2\alpha)}{\sin \frac{1}{2}(\theta - \beta) \cos \frac{1}{2}\theta} \right|. \quad \dots \quad \dots \quad \dots \quad \dots \quad (56)$$

Also

$$\frac{q_{am}}{q_{0m}} = \left| \frac{\cos \frac{1}{2}(\theta - \gamma - 2\alpha)}{\cos \frac{1}{2}(\theta - \gamma)} \right|, \quad \dots \quad \dots \quad \dots \quad \dots \quad \dots \quad (57)$$

provided  $m$  is so adjusted that  $\gamma$  is unchanged, as  $\alpha$  varies.

Consider the following velocity distribution.

$$\log q_0 = \left\{ \begin{array}{ll} \log \left| \frac{\sin \frac{1}{2}(\theta - \beta) \cos \frac{1}{2}\theta}{\sin \frac{1}{2}(\theta - \beta + \gamma) \cos \frac{1}{2}(\theta - \gamma)} \right|, & 0 < \theta < 2\pi \\ + \log \left| \frac{\cos \frac{1}{2}(\theta - \gamma)}{\cos \frac{1}{2}(\theta - \gamma - 2\alpha)} \right|, & \alpha + \gamma < \theta < \pi + \alpha + \gamma \\ + S & 0 < \theta < 2\pi. \end{array} \right\} \quad \dots \quad (58)$$

By equations (56) and (57),  $S$  is the value of  $\log q_{am}$  on the upper surface and of  $q_{0m}$  on the lower surface. The conjugates of the first two terms of equation (58) are given in Appendix I. It is thus possible to design an aerofoil in which the velocity with suction is prescribed right into the slot. The slot shape is worked out with the rest of the aerofoil, depending chiefly on the type of velocity distribution assumed in the slot mouth. For thick suction aerofoils with the slot well back on the chord, as those in Figs. 2 and 3, the modifications of shape through use of the method are probably small.

*7. Practical Notes.*—All the necessary material for satisfactorily designing aerofoils to fill a wide range of requirements has now been set out and explained. It remains to consider various practical difficulties which may be encountered while actually carrying out the design.

The method can very easily provide velocity distributions which, at a certain incidence, are either flat or changing steadily along the chord. In the first case  $\log q$  is made constant over a suitable range of  $\theta$ , and in the second it is made proportional to  $\cos \theta$ . As pointed out earlier,  $x$  varies along the chord like  $\cos \theta$ , to a good approximation. There should of course be no discontinuities in the  $\log q$  chosen, except at the slot of a suction aerofoil, and discontinuities in  $d(\log q)/d\theta$  should be avoided as far as possible. It is difficult to obtain any required thickness exactly. The chief factor controlling the thickness is the extent of the incidence range, the two being roughly proportional for a given type of velocity distribution. It is always necessary to satisfy equation (23), and for this purpose enough parameters in  $\log q_0$  must be left arbitrary. If it is desired to prescribe the pitching moment, another parameter must be included to enable equation (28) to be satisfied. For  $C_{M0}$  other than zero, the value of the chord  $c$  must be guessed. This can usually be done with sufficient accuracy. When the equations have been solved and the values of the parameters determined, the velocity distribution over the aerofoil can be worked out. From the maximum velocity it can often be decided what the thickness is likely to be, making use of previous experience. If the calculated value is unsatisfactory, it is a waste of time to proceed further with working out the aerofoil shape. The form assumed for  $\log q_0$  must be adjusted, and equation (23) solved afresh, until a satisfactory velocity distribution is obtained.

The conjugate  $\chi$  is now found. If  $\log q_0$  has been chosen in terms of the functions in Appendix I, this presents no difficulty. Next, the integrands in equation (11) must be calculated at intervals of  $\theta$  suitable for numerical integration. For an aerofoil to be used in practice, seven figure tables should be used, and a calculating machine is essential. It is convenient to have available tables of  $\cos \theta$  and  $\log \sin \frac{1}{2} \theta$  tabulated to seven decimal places, for integral values of  $\theta$  in degrees. Factors of  $\chi$  or other terms of the integrand, constant over the whole range of  $\theta$  may be omitted, but care must be taken to take account of them when evaluating the chord  $c$  and the no-lift angle. In regions where there is a singularity in  $\log q_0$ , for example at the leading edge or near a suction slot, the interval of tabulation should be reduced. Simpson's rule may then be used throughout the integration to find the aerofoil shape. This is easily carried out on an adding machine. Methods of integration involving the repeated taking of differences break down owing to the awkward behaviour of the differences near the singularity, and it is easier to calculate a few extra points than to develop and apply a special rule. Simpson's rule of integration in the form

$$\frac{3}{a} \int_0^{2a} y \, dx = y_0 + 4y_a + y_{2a} \quad \dots \quad \dots \quad \dots \quad \dots \quad \dots \quad (59)$$

gives the co-ordinates at even points of tabulation only. An application of the cubic rule in the form

$$\frac{3}{a} \int_0^{3a} y \, dx = \frac{9}{8} \{y_0 + 3y_a + 3y_{2a} + y_{3a}\} \quad \dots \quad \dots \quad \dots \quad (60)$$

gives an odd point, and the co-ordinates of the remaining odd points follow by Simpson's rule. The cubic rule may also usefully be used to check the integrations. The accuracy of the whole work is shown by whether the aerofoil contour closes up on integrating round the circle. Very small errors may be smoothed out over the surface.

The sign of the integrand in equation (11) must be viewed with suspicion. The difficulty is that  $\chi$  has been defined in two ways, firstly as the direction of the velocity  $q$ , and secondly as the tangent to the aerofoil in the direction of  $\theta$  increasing. These two expressions may differ by  $\pi$ . At a stagnation point the former alters by  $\pi$  while the latter is unchanged, while at a cusped trailing edge the reverse is true. In practice there is never any difficulty in deciding by inspection which sign must be taken in equation (11) to get the aerofoil contour.

On a suction aerofoil, the integration breaks down near each velocity discontinuity. If there is just one such point on the aerofoil, it is possible to integrate towards it from both directions, but the slot position and the accuracy of joining up are not determined. If there are two or more slots, the integration should be carried out over as much of the surface as possible, introducing arbitrary constants where necessary.

For a discontinuity  $k$  in  $\log g_0$  at  $\theta = \beta$ , the value of  $\chi$  in the neighbourhood may be written

$$\chi = \chi_0 + \frac{k}{\pi} \log |\theta - \beta| \quad \dots \quad \dots \quad \dots \quad \dots \quad \dots \quad \dots \quad (61)$$

where  $\chi_0$  is continuous near  $\theta = \beta$ . By equation (9),  $ds/d\theta = (2 \sin \theta)/q_0$ , so if  $s$  is measured from the discontinuity and is small,

which is the equation of a logarithmic spiral, if variations in  $\chi_1$  are ignored.  $\chi_1$  has a discontinuity of  $k^2/\pi$  at  $\theta = \pi$ , so the two branches of the spiral are relatively displaced. If  $k^2/\pi = \pi$  the branches coincide, and it follows as an interesting corollary that the maximum velocity discontinuity theoretically possible is  $e^\pi$ .

The theory of the logarithmic spiral can now be applied to provide the following relations. If the aerofoil co-ordinates at  $\theta = \beta + n\delta$ , where  $\delta$  is the interval of tabulation, assumed small, are  $z_n = x_n + iy_n$ , then

$$\arg \{z_n - z_{-n}\} = \chi_n - \tan^{-1} \frac{k}{\pi}, \quad \dots \quad \dots \quad \dots \quad \dots \quad \dots \quad \dots \quad (64)$$

where  $\chi_n$  is the mean of the values of  $\chi$  at  $\theta = \beta - n\delta$  and  $\theta = \beta + n\delta$ . For a true logarithmic spiral these two values would be equal, and this provides an indication if  $\delta$  has been taken small enough. Also

The slot position  $z_0$  lies on the line joining  $z_{-n}$  and  $z_{+n}$ , at the point dividing it in the ratio  $e^k : 1$ , as is seen from equation (62).

This relation, together with equation (64) for  $n = 1$  and for  $n = 2$ , and equation (65) for  $n = 1, m = 2$ , usually provides all the material necessary to complete the integration and check that the contour closes up. Clearly the points  $z_n$  must be so near the slot that the approximation to a logarithmic spiral is a close one.

This completes the calculation of the profile. The chord is measured, and the aerodynamic characteristics of the aerofoil can now be deduced. Several examples are worked out fully in R. & M. 2112<sup>1</sup>, and other sections designed on the method are shown in R. & M. 2162<sup>3</sup> and 2111<sup>4</sup>. In Appendix IV the design of one particular cambered suction aerofoil is considered in detail, as an illustration of the various points treated above.

## APPENDIX I

### *List of Conjugates*

For a function  $f(\theta)$ , periodic in  $\theta$  with period  $2\pi$ , the Fourier conjugate function  $G(\theta)$  is given by Poisson's integral as

$$G(\theta) = \frac{1}{2\pi} \int_{-\pi}^{\pi} f(\phi) \cot \frac{1}{2}(\theta - \phi) d\phi .$$

If  $f(\theta)$  is an even function of  $\theta$ , this takes the simpler form

$$G(\theta) = -\frac{\sin \theta}{\pi} \int_0^\pi \frac{f(\phi)}{\cos \theta - \cos \phi} d\phi ,$$

while if  $f(\theta)$  is an odd function of  $\theta$  it becomes

$$G(\theta) = -\frac{1}{\pi} \int_0^\pi \frac{f(\phi) \sin \phi}{\cos \theta - \cos \phi} d\phi .$$

The integrals for the first few Fourier constants of  $f(\theta)$ , which are required for various purposes in the aerofoil design are

$$A = \int_{-\pi}^{\pi} f(\theta) d\theta ,$$

$$B = \int_{-\pi}^{\pi} f(\theta) \cos \theta d\theta ,$$

$$C = \int_{-\pi}^{\pi} f(\theta) \sin \theta d\theta ,$$

$$D = \int_{-\pi}^{\pi} f(\theta) \cos 2\theta d\theta ,$$

$$E = \int_{-\pi}^{\pi} f(\theta) \sin 2\theta d\theta .$$

These five expressions and  $G(\theta)$  are tabulated below for a large number of functions  $f(\theta)$ . The terms of  $G$  enclosed in square brackets are independent of  $\theta$ , and may often be omitted. In many cases reference is made to the appropriate section of Appendix II, where the method of evaluating the integrals is demonstrated. Where no such reference is made the integrations are of a trivial nature.

The functions

$$F(T) = \frac{2}{\pi} \int_0^T \frac{\log x}{x^2 - 1} dx , \quad \text{and}$$

$X(\theta) = -\frac{1}{\pi} \int_0^\theta \log \sin \frac{1}{2}t dt$ , occur frequently. These functions are tabulated in Tables 1 and 2 respectively.

1.  $k, \lambda < \theta < \mu$

$$G = \frac{k}{\pi} \log \left| \frac{\sin \frac{1}{2}(\theta - \lambda)}{\sin \frac{1}{2}(\theta - \mu)} \right|$$

$$A = k(\mu - \lambda)$$

$$B = k(\sin \mu - \sin \lambda)$$

$$C = k(\cos \lambda - \cos \mu)$$

$$D = \frac{1}{2}k(\sin 2\mu - \sin 2\lambda)$$

$$E = \frac{1}{2}k(\cos 2\lambda - \cos 2\mu)$$

$$2. \quad \cos \theta, \lambda < \theta < \mu \quad G = \frac{\mu - \lambda}{2\pi} \sin \theta + \frac{\cos \theta}{\pi} \log \left| \frac{\sin \frac{1}{2}(\theta - \lambda)}{\sin \frac{1}{2}(\theta - \mu)} \right|$$

$$+ \left[ \frac{1}{2\pi} (\cos \lambda - \cos \mu) \right]$$

$$A = \sin \mu - \sin \lambda$$

$$B = \frac{1}{4} \{2(\mu - \lambda) + \sin 2\mu - \sin 2\lambda\}$$

$$C = \frac{1}{4} \{\cos 2\lambda - \cos 2\mu\}$$

$$D = \frac{1}{6} \{\sin 3\mu + 3 \sin \mu - \sin 3\lambda - 3 \sin \lambda\}$$

$$E = \frac{1}{6} \{\cos 3\lambda + 3 \cos \lambda - \cos 3\mu - 3 \cos \mu\}$$

$$3. \quad \sin \theta, \lambda < \theta < \mu \quad G = -\frac{\mu - \lambda}{2\pi} \cos \theta + \frac{\sin \theta}{\pi} \log \left| \frac{\sin \frac{1}{2}(\theta - \lambda)}{\sin \frac{1}{2}(\theta - \mu)} \right|$$

$$+ \left[ \frac{1}{2\pi} (\sin \lambda - \sin \mu) \right]$$

$$A = \cos \lambda - \cos \mu$$

$$B = \frac{1}{4} \{\cos 2\lambda - \cos 2\mu\}$$

$$C = \frac{1}{4} \{2(\mu - \lambda) - \sin 2\mu + \sin 2\lambda\}$$

$$D = \frac{1}{6} \{\cos 3\lambda - 3 \cos \lambda - \cos 3\mu + 3 \cos \mu\}$$

$$E = \frac{1}{6} \{3 \sin \mu - \sin 3\mu - 3 \sin \lambda + \sin 3\lambda\}$$

$$4. \quad \cos 2\theta, \lambda < \theta < \mu \quad G = \frac{\mu - \lambda}{2\pi} \sin \theta + \frac{2}{\pi} \sin \frac{\mu - \lambda}{2} \sin \left( \theta + \frac{\mu - \lambda}{2} \right)$$

$$+ \frac{\cos 2\theta}{\pi} \log \left| \frac{\sin \frac{1}{2}(\theta - \lambda)}{\sin \frac{1}{2}(\theta - \mu)} \right| + \left[ \frac{1}{4\pi} (\cos 2\lambda - \cos 2\mu) \right]$$

$$A = \frac{1}{2} \{\sin 2\mu - \sin 2\lambda\}$$

$$B = \frac{1}{6} \{\sin 3\mu + 3 \sin \mu - \sin 3\lambda - 3 \sin \lambda\}$$

$$C = \frac{1}{6} \{\cos 3\lambda - 3 \cos \lambda - \cos 3\mu + 3 \cos \mu\}$$

$$D = \frac{1}{8} \{4(\mu - \lambda) + \sin 4\mu - \sin 4\lambda\}$$

$$E = \frac{1}{8} \{\cos 4\lambda - \cos 4\mu\}$$

5.  $\sin 2\theta, \lambda < \theta < \mu$        $G = -\frac{\mu - \lambda}{2\pi} \cos 2\theta - \frac{2}{\pi} \sin \frac{\mu - \lambda}{2} \cos \left(\theta + \frac{\mu + \lambda}{2}\right)$

$$+ \frac{\sin 2\theta}{\pi} \log \left| \frac{\sin \frac{1}{2}(\theta - \lambda)}{\sin \frac{1}{2}(\theta - \mu)} \right| + \left[ \frac{1}{4\pi} (\sin 2\lambda - \sin 2\mu) \right]$$

$$A = \frac{1}{2} \{\cos 2\lambda - \cos 2\mu\}$$

$$B = \frac{1}{6} \{\cos 3\lambda + 3 \cos \lambda - \cos 3\mu - 3 \cos \mu\}$$

$$C = \frac{1}{6} \{3 \sin \mu - \sin 3\mu - 3 \sin \lambda + \sin 3\lambda\}$$

$$D = \frac{1}{8} \{\cos 4\lambda - \cos 4\mu\}$$

$$E = \frac{1}{8} \{4(\mu - \lambda) - \sin 4\mu + \sin 4\lambda\}$$

6.  $\cos 3\theta, \lambda < \theta < \mu$        $G = \frac{\mu - \lambda}{2\pi} \sin 3\theta + \frac{2}{\pi} \sin \frac{\mu - \lambda}{2} \sin \left(2\theta + \frac{\lambda + \mu}{2}\right)$

$$+ \frac{2}{\pi} \sin 2(\mu - \lambda) \sin (\theta + \lambda + \mu)$$

$$+ \frac{\cos 3\theta}{\pi} \log \left| \frac{\sin \frac{1}{2}(\theta - \lambda)}{\sin \frac{1}{2}(\theta - \mu)} \right| + \left[ \frac{1}{6\pi} (\cos 3\lambda - \cos 3\mu) \right]$$

$$A = \frac{1}{3} \{\sin 3\mu - \sin 3\lambda\}$$

$$B = \frac{1}{8} \{\sin 4\mu + 2 \sin 2\mu - \sin 4\lambda - 2 \sin 2\lambda\}$$

$$C = \frac{1}{8} \{\cos 4\lambda - 2 \cos 2\lambda - \cos 4\mu + 2 \cos 2\mu\}$$

$$D = \frac{1}{10} \{\sin 5\mu + 5 \sin \mu - \sin 5\lambda - 5 \sin \lambda\}$$

$$E = \frac{1}{10} \{\cos 5\lambda - 5 \cos \lambda - \cos 5\mu + 5 \cos \mu\}$$

7.  $\sin 3\theta, \lambda < \theta < \mu$        $G = -\frac{\mu - \lambda}{2\pi} \cos 3\theta - \frac{2}{\pi} \sin \frac{\mu - \lambda}{2} \cos \left(2\theta + \frac{\lambda + \mu}{2}\right)$

$$- \frac{2}{\pi} \sin 2(\mu - \lambda) \cos (\theta + \lambda + \mu)$$

$$+ \frac{\sin 3\theta}{\pi} \log \left| \frac{\sin \frac{1}{2}(\theta - \lambda)}{\sin \frac{1}{2}(\theta - \mu)} \right| + \left[ \frac{1}{6\pi} (\sin 3\lambda - \sin 3\mu) \right]$$

$$A = \frac{1}{3} \{\cos 3\lambda - \cos 3\mu\}$$

$$B = \frac{1}{8} \{\cos 4\lambda + 2 \cos 2\lambda - \cos 4\mu - 2 \cos 2\mu\}$$

$$C = \frac{1}{8} \{2 \sin 2\mu - \sin 4\mu - 2 \sin 2\lambda + \sin 4\lambda\}$$

$$D = \frac{1}{16} \{\cos 5\lambda + 5 \cos \lambda - \cos 5\mu - 5 \cos \mu\}$$

$$E = \frac{1}{16} \{5 \sin \mu - \sin 5\mu - 5 \sin \lambda + \sin 5\lambda\}$$

8.  $\theta, \lambda < \theta < \mu$

$$G = \frac{\lambda}{\pi} \log \left| \sin \frac{1}{2}(\theta - \lambda) \right| - \frac{\mu}{\pi} \log \left| \sin \frac{1}{2}(\theta - \mu) \right|$$

$$- X(\theta - \lambda) + X(\theta - \mu)$$

$$A = \frac{1}{2}(\mu^2 - \lambda^2)$$

$$B = \mu \sin \mu + \cos \mu - \lambda \sin \lambda - \cos \lambda$$

$$C = \lambda \cos \lambda - \sin \lambda - \mu \cos \mu + \sin \mu$$

$$D = \frac{1}{4} \{2\mu \sin 2\mu + \cos 2\mu - 2\lambda \sin 2\lambda - \cos 2\lambda\}$$

$$E = \frac{1}{4} \{2\lambda \cos 2\lambda - \sin 2\lambda - 2\mu \cos 2\mu + \sin 2\mu\}$$

9.  $\cos \frac{1}{2}\theta, \lambda < \theta < \mu$

$$G = \frac{\cos \frac{1}{2}\theta}{\pi} \log \left| \frac{\tan \frac{1}{4}(\theta - \lambda)}{\tan \frac{1}{4}(\theta - \mu)} \right| + \left[ \frac{1}{\pi} (\cos \frac{1}{2}\lambda - \cos \frac{1}{2}\mu) \right]$$

$$A = 2 \{\sin \frac{1}{2}\mu - \sin \frac{1}{2}\lambda\}$$

$$B = \frac{1}{3} \{\sin \frac{3}{2}\mu - \sin \frac{3}{2}\lambda\} + \sin \frac{1}{2}\mu - \sin \frac{1}{2}\lambda$$

$$C = \frac{1}{3} \{\cos \frac{3}{2}\lambda - \cos \frac{3}{2}\mu\} + \cos \frac{1}{2}\lambda - \cos \frac{1}{2}\mu$$

$$D = \frac{1}{5} \{\sin \frac{5}{2}\mu - \sin \frac{5}{2}\lambda\} + \frac{1}{3} \{\sin \frac{3}{2}\mu - \sin \frac{3}{2}\lambda\}$$

$$E = \frac{1}{5} \{\cos \frac{5}{2}\lambda - \cos \frac{5}{2}\mu\} + \frac{1}{3} \{\cos \frac{3}{2}\lambda - \cos \frac{3}{2}\mu\}$$

10.  $\sin \frac{1}{2}\theta, \lambda < \theta < \mu$

$$G = \frac{\sin \frac{1}{2}\theta}{\pi} \log \left| \frac{\tan \frac{1}{4}(\theta - \lambda)}{\tan \frac{1}{4}(\theta - \mu)} \right| + \left[ \frac{1}{\pi} (\sin \frac{1}{2}\lambda - \sin \frac{1}{2}\mu) \right]$$

$$A = 2 \{\cos \frac{1}{2}\lambda - \cos \frac{1}{2}\mu\}$$

$$B = \frac{1}{3} \{\cos \frac{3}{2}\lambda - \cos \frac{3}{2}\mu\} - \cos \frac{1}{2}\lambda + \cos \frac{1}{2}\mu$$

$$C = \sin \frac{1}{2}\mu - \sin \frac{1}{2}\lambda - \frac{1}{3} \{\sin \frac{3}{2}\mu - \sin \frac{3}{2}\lambda\}$$

$$D = \frac{1}{5} \{\cos \frac{5}{2}\lambda - \cos \frac{5}{2}\mu\} - \frac{1}{3} \{\cos \frac{3}{2}\lambda - \cos \frac{3}{2}\mu\}$$

$$E = \frac{1}{5} \{\sin \frac{3}{2}\mu - \sin \frac{3}{2}\lambda\} - \frac{1}{3} \{\sin \frac{5}{2}\mu - \sin \frac{5}{2}\lambda\}$$

11.  $\left\{ -1 - \sin 6\theta, -\frac{\pi}{12} < \theta < 0 ; 1 - \sin 6\theta, 0 < \theta < \frac{\pi}{12} \right\} = P_6(\theta)$

$G = Q_6(\theta)$  This is worked out in Appendix II, section 3, and tabulated in Table 5.

$$A = 0$$

$$B = 0$$

$$C = 2 \left[ 1 - \frac{36}{35} \cos \frac{\pi}{12} \right] = 0.0129526$$

$$D = 0$$

$$E = 1 - \frac{9}{8} \cos \frac{\pi}{6} = 0.0257214$$

12.  $\log \tan \frac{1}{2}\theta$ ,  $-\mu < \theta < \mu$  This is considered in Appendix II, section 3.

$$G = -F\left(\tan \frac{\mu}{2} \cot \frac{\theta}{2}\right) + \frac{\log \tan \frac{1}{2}\theta}{\pi} \log \left| \frac{\sin \frac{1}{2}(\theta + \mu)}{\sin \frac{1}{2}(\theta - \mu)} \right|$$

$$A = -2\pi \{X(\mu) + X(\pi - \mu) - X(\pi)\}$$

$$B = 2 \sin \mu \log \tan \frac{1}{2}\mu - 2\mu$$

$$C = 0$$

$$D = \sin 2\mu \log \tan \frac{1}{2}\mu - 2 \sin \mu$$

$$E = 0$$

13.  $\log \sin \theta$ ,  $-\frac{\pi}{2} < \theta < \frac{\pi}{2}$  This is considered in Appendix II, section 4.

$$G = \frac{1}{2}\theta - \frac{1}{2}F\left[\tan^2 \frac{1}{2}\left(\theta - \frac{\pi}{2}\right)\right] + \frac{\pi}{8} \pm \frac{\pi}{2}$$

$$A = -\pi \log 2$$

$$B = -2$$

$$C = 0$$

$$D = -\frac{\pi}{2}$$

$$E = 0$$

14.  $\log \left| \frac{\sin \frac{1}{2}(\theta + \mu)}{\sin \frac{1}{2}(\theta - \mu)} \right|$  This is considered in Appendix II, section 5.

$$G = 0 + [\mu]$$

$$A = 0$$

$$B = 0$$

$$C = 2\pi \sin \mu$$

$$D = 0$$

$$E = \pi \sin 2\mu$$

15.  $\log \left| \frac{\sin \frac{1}{2}(\theta - \lambda)}{\sin \frac{1}{2}(\theta - \mu)} \right|$  This follows directly from section 14, above.

$$G = 0 + [\frac{1}{2}(\mu - \lambda)]$$

$$A = 0$$

$$B = \pi(\cos \mu - \cos \lambda)$$

$$C = \pi(\sin \mu - \sin \lambda)$$

$$D = \frac{1}{2}\pi(\cos 2\mu - \cos 2\lambda)$$

$$E = \frac{1}{2}\pi(\sin 2\mu - \sin 2\lambda)$$

16.  $\log \left| \frac{\cos (\frac{1}{2}\theta - \alpha_2)}{\cos (\frac{1}{2}\theta - \alpha_1)} \right|$  This is section 15 in another form.

$$G = 0 + [\alpha_1 - \alpha_2]$$

$$A = 0$$

$$B = \pi(\cos 2\alpha_2 - \cos 2\alpha_1)$$

$$C = \pi(\sin 2\alpha_2 - \sin 2\alpha_1)$$

$$D = \frac{1}{2}\pi(\cos 4\alpha_1 - \cos 4\alpha_2)$$

$$E = \frac{1}{2}\pi(\sin 4\alpha_1 - \sin 4\alpha_2)$$

17.  $\log \left| \frac{\cos \frac{\theta}{2}}{\cos \left( \frac{\theta}{2} - \alpha \right)} \right|, \quad 0 < \theta < \pi,$  continued as an even function of  $\theta$ .

See Appendix II, section 6.

$$G = F(\tan \alpha \tan \frac{1}{2}\theta)$$

$$A = -2\pi \{X(2\alpha) + X(\pi - 2\alpha) - X(\pi)\} = 4 \int_0^{\tan \alpha} \frac{\log x}{1+x^2} dx$$

$$B = 2(\pi \sin^2 \alpha + \sin 2\alpha \log \cot \alpha)$$

$$C = 0$$

$$D = 2 \sin 2\alpha - \pi \sin^2 2\alpha - \sin 4\alpha \log \cot \alpha$$

$$E = 0$$

18.  $\log \left| \frac{\cos \frac{\theta}{2}}{\cos \left( \frac{\theta}{2} - \alpha \right)} \right|, \quad \alpha < \theta < \pi + \alpha$  This is deduced from sections 16 and 17.

$$G = F \{ \tan \frac{1}{2}\alpha \tan \frac{1}{2}(\theta - \alpha) \} + [\frac{1}{2}\alpha]$$

$$A = -2\pi \{ X(\alpha) + X(\pi - \alpha) - X(\pi) \}$$

$$B = 2 \sin \alpha \cos \alpha \log \cot \frac{1}{2}\alpha + \pi \sin^2 \alpha$$

$$C = 2 \sin^2 \alpha \log \cot \frac{1}{2}\alpha - \pi \sin \alpha \cos \alpha$$

$$D = 2 \sin \alpha \cos 2\alpha - \frac{1}{2}\pi \sin^2 2\alpha - \frac{1}{2} \sin 4\alpha \log \cot \frac{1}{2}\alpha$$

$$E = 2 \sin \alpha \sin 2\alpha + \frac{1}{4}\pi \sin 4\alpha - \sin^2 2\alpha \log \cot \frac{1}{2}\alpha$$

19.  $\log \left| \frac{\cos \frac{\theta - \gamma}{2}}{\cos \left( \frac{\theta - \gamma}{2} - \alpha \right)} \right|, \quad \alpha + \gamma < \theta < \pi + \alpha + \gamma.$

This follows at once from section 18.

$$G = F \{ \tan \frac{1}{2}\alpha \tan \frac{1}{2}(\theta - \alpha - \gamma) \} + [\frac{1}{2}\alpha]$$

$$A = -2\pi \{ X(\alpha) + X(\pi - \alpha) - X(\pi) \}$$

$$B = 2 \sin \alpha \cos (\alpha + \gamma) \log \cot \frac{1}{2}\alpha + \pi \sin \alpha \sin (\alpha + \gamma)$$

$$C = 2 \sin \alpha \sin (\alpha + \gamma) \log \cot \frac{1}{2}\alpha - \pi \sin \alpha \cos (\alpha + \gamma)$$

$$D = 2 \sin \alpha \cos 2(\alpha + \gamma) - \frac{1}{2}\pi \sin 2\alpha \sin 2(\alpha + \gamma)$$

$$- \sin 2\alpha \cos 2(\alpha + \gamma) \log \cot \frac{1}{2}\alpha$$

$$E = 2 \sin \alpha \sin 2(\alpha + \gamma) + \frac{1}{2}\pi \sin 2\alpha \cos 2(\alpha + \gamma)$$

$$- \sin 2\alpha \sin 2(\alpha + \gamma) \log \cot \frac{1}{2}\alpha$$

20.  $\log \left| \frac{\cos \frac{\theta}{2}}{\cos \left( \frac{\theta}{2} - \alpha_1 \right)} \right|, \quad \alpha_1 + \alpha_2 < \theta < \pi + \alpha_1 + \alpha_2; + \log \left| \frac{\cos \frac{\theta}{2}}{\cos \left( \frac{\theta}{2} - \alpha_2 \right)} \right|,$

$-\pi + \alpha_1 + \alpha_2 < \theta < \alpha_1 + \alpha_2$ . This is a combination of sections 16 and 19.

Write  $\alpha_1 - \alpha_2 = 2\alpha_0$ .

$$G = F \{ \tan \alpha_0 \tan \frac{1}{2}(\theta - \alpha_1 - \alpha_2) \} + [\frac{1}{2}(\alpha_1 + \alpha_2)]$$

$$A = -2\pi \{ X(2\alpha_0) + X(\pi - 2\alpha_0) - X(\pi) \}$$

$$B = \{ \sin 2\alpha_1 - \sin 2\alpha_2 \} \log \cot \alpha_0 + \frac{1}{2}\pi \{ 2 - \cos 2\alpha_1 - \cos 2\alpha_2 \}$$

$$\begin{aligned}
C &= \{\cos 2\alpha_2 - \cos 2\alpha_1\} \log \cot \alpha_0 - \frac{1}{2}\pi \{\sin 2\alpha_1 + \sin 2\alpha_2\} \\
D &= 2 \sin 2\alpha_0 \cos 2(\alpha_1 + \alpha_2) - \frac{1}{4}\pi \{2 - \cos 4\alpha_1 - \cos 4\alpha_2\} \\
&\quad - \frac{1}{2} \{\sin 4\alpha_1 - \sin 4\alpha_2\} \log \cot \alpha_0 \\
E &= 2 \sin 2\alpha_0 \sin 2(\alpha_1 + \alpha_2) + \frac{1}{4}\pi \{\sin 4\alpha_1 + \sin 4\alpha_2\} \\
&\quad - \frac{1}{2} \{\cos 4\alpha_2 - \cos 4\alpha_1\} \log \cot \alpha_0
\end{aligned}$$


---

## APPENDIX II

### *Evaluation of Conjugates*

The notation of Appendix I is used throughout.

1.  $G$  is readily evaluated for the functions of Appendix I, section 2, to Appendix I, section 7, inclusive, by writing  $f(t) = \{f(t) - f(\theta)\} + f(\theta)$ . The bracketed term is then divisible by  $\sin \frac{1}{2}(\theta - t)$ .

For example, in Appendix I, section 2,

$$\begin{aligned}
G(\theta) &= \frac{1}{2\pi} \int_{\lambda}^{\mu} \cos t \cot \frac{1}{2}(\theta - t) dt \\
&= \frac{1}{2\pi} \int_{\lambda}^{\mu} (\cos \theta - \cos t) \cot \frac{1}{2}(\theta - t) dt + \frac{1}{2\pi} \int_{\lambda}^{\mu} \cos \theta \cot \frac{1}{2}(\theta - t) dt \\
&= \frac{\mu - \lambda}{2\pi} \sin \theta + \frac{1}{2\pi} (\cos \lambda - \cos \mu) + \frac{\cos \theta}{\pi} \log \left| \frac{\sin \frac{1}{2}(\theta - \lambda)}{\sin \frac{1}{2}(\theta - \mu)} \right|.
\end{aligned}$$

For Appendix I, section 9, write

$$\cos \frac{1}{2}t = \cos \frac{1}{2}(\theta - t) \cos \frac{1}{2}\theta + \sin \frac{1}{2}(\theta - t) \sin \frac{1}{2}\theta,$$

and  $G$  can easily be found. A similar technique is used for Appendix I, section 10.

2. Appendix I, section 11, consists of the trailing-edge term, an odd function of  $\theta$ . The conjugate  $Q_6$  is made up of

$$\begin{aligned}
&\frac{1}{\pi} \log \left| \frac{\sin \frac{1}{2}\theta}{\sin \frac{1}{2}(\theta + \frac{\pi}{12})} \right| - \frac{1}{\pi} \log \left| \frac{\sin \frac{1}{2}(\theta - \frac{\pi}{12})}{\sin \frac{1}{2}\theta} \right|, \\
&= \frac{1}{\pi} \left\{ 2 \log \left| \sin \frac{1}{2}\theta \right| - \log \left| \sin \frac{1}{2}(\theta + \frac{\pi}{12}) \right| - \log \left| \sin \frac{1}{2}(\theta - \frac{\pi}{12}) \right| \right\},
\end{aligned}$$

and of

$$\begin{aligned}
& \frac{1}{\pi} \int_0^{\pi/12} \frac{\sin 6t \sin t}{\cos \theta - \cos t} dt \\
&= \frac{1}{2\pi} \int_0^{\pi/12} \frac{\cos 5t - \cos 7t}{\cos \theta - \cos t} dt \\
&= \frac{1}{2\pi} \left\{ I_5\left(\frac{\pi}{12}\right) - I_7\left(\frac{\pi}{12}\right) \right\}, \quad \text{as given in Ref. 2, Lemma 4.}
\end{aligned}$$

$$\begin{aligned}
\text{Hence } Q_6 &= \frac{1}{\pi} \left\{ 2 \log \left| \sin \frac{1}{2}\theta \right| - (1 + \sin 6\theta) \log \left| \sin \frac{1}{2}(\theta + \frac{\pi}{12}) \right| \right. \\
&\quad \left. - (1 - \sin 6\theta) \log \left| \sin \frac{1}{2}(\theta - \frac{\pi}{12}) \right| + \frac{1}{6} + \frac{\pi}{12} \cos 6\theta + 2 \sum_{s=1}^5 \frac{\sin(6-s)\frac{\pi}{12}}{6-s} \cos s\theta \right\}
\end{aligned}$$

This is tabulated against  $\theta$  in Table 5.

The Fourier constants are easily found, and are listed in Appendix I, section 11.

3. The conjugate of  $\log \tan \frac{1}{2}\theta$ ,  $-\mu < \theta < \mu$ , an even function of  $\theta$ , is

$$G(\theta) = -\frac{\sin \theta}{\pi} \int_0^\mu \frac{\log \tan \frac{1}{2}\phi}{\cos \theta - \cos \phi} d\phi.$$

Write  $t = \tan \frac{1}{2}\theta$ ,  $\phi = \tan \frac{1}{2}\phi$ ,

$$m = \tan \frac{1}{2}\mu.$$

$$\text{Then } G = -\frac{2t}{\pi} \int_0^m \frac{\log \phi}{\phi^2 - t^2} d\phi$$

$$\begin{aligned}
&= -F\left(\frac{m}{t}\right) - \frac{2}{\pi} \log t \int_0^{mt} \frac{dx}{x^2 - 1}, \quad \text{writing } \frac{\phi}{t} = x \\
&= -F(\tan \frac{1}{2}\mu \cot \frac{1}{2}\theta) + \frac{1}{\pi} \log \tan \frac{1}{2}\theta \log \left| \frac{\sin \frac{1}{2}(\theta + \mu)}{\sin \frac{1}{2}(\theta - \mu)} \right|.
\end{aligned}$$

4.  $\log |\sin \theta|$ ,  $-\frac{\pi}{2} < \theta < \frac{\pi}{2}$ , is an even function of  $\theta$ .

$$G(\theta) = -\frac{\sin \theta}{\pi} \int_0^{\pi/2} \frac{\log \sin \phi}{\cos \theta - \cos \phi} d\phi.$$

Write  $\phi = \tan \frac{1}{2}\theta$ ,  $t = \tan \frac{1}{2}\theta$ . Then as in the previous section,

$$G = \frac{1}{\pi} \int_0^1 \frac{\phi^2 - 1}{\phi(\phi^2 + 1)} \log \left| \frac{\phi + t}{\phi - t} \right| d\phi,$$

$$\begin{aligned}
\frac{dG}{dt} &= \frac{2}{\pi} \int_0^1 \frac{\phi^2 - 1}{(\phi^2 + 1)(\phi^2 - t^2)} d\phi \\
&= \frac{1}{\pi} \cdot \frac{t^2 - 1}{t(t^2 + 1)} \log \left| \frac{t - 1}{t + 1} \right| + \frac{1}{1 + t^2}.
\end{aligned}$$

Hence 
$$G = \frac{1}{\pi} \int \frac{t^2 - 1}{t(t^2 + 1)} \log \left| \frac{t-1}{t+1} \right| dt + \tan^{-1} t$$
  

$$= G_1 + \frac{1}{2}\theta .$$

Writing successively  $t = \tan \frac{1}{2}\theta$ ,  $\theta - \frac{\pi}{2} = \theta_1$ ,  $\tan \frac{1}{2}\theta_2 = t_1$ ,  $t_1^2 = x$ ,

$$G_1 = -\frac{1}{2}F\left\{\tan^2 \frac{1}{2}\left(\theta - \frac{\pi}{2}\right)\right\} .$$

Thus  $G = \frac{1}{2}\theta - \frac{1}{2}F\left\{\tan^2 \frac{1}{2}\left(\theta - \frac{\pi}{2}\right)\right\} + \frac{\pi}{8} \pm \frac{\pi}{2} .$

At  $\theta = 0$ ,  $G$  has a discontinuity of  $-\pi$ . The arbitrary constant is chosen so that  $G = \pm \pi/2$  at  $\theta = 0$ .

5. From Appendix I, section 1, the conjugate of  $k$ ,  $-\mu < \theta < \mu$  is  $\frac{k}{\pi} \log \left| \frac{\sin \frac{1}{2}(\theta + \mu)}{\sin \frac{1}{2}(\theta - \mu)} \right|$ .

Now if  $f(\theta)$  is the conjugate of  $g(\theta)$ , the conjugate of  $g(\theta)$  is  $-f(\theta)$ .

Hence the conjugate of  $\log \left| \frac{\sin \frac{1}{2}(\theta + \mu)}{\sin \frac{1}{2}(\theta - \mu)} \right|$  is  $-\pi$ ,  $-\mu < \theta < \mu$ . Since the average value must be zero, to this must be added  $2\mu \cdot \pi/2\pi = \mu$ .

Further, since changes of  $\pi$  in  $\chi$  are unimportant, the value of  $G$  may be taken as  $\mu$  everywhere.

This conjugate may be evaluated directly, but the work is laborious.

Since the function is odd,  $A = B = D = 0$ .  $C$  and  $E$  are easily found, making use of the relation

$$\int_0^\pi \frac{\cos n\theta}{\cos \theta - \cos \mu} d\theta = \pi \frac{\sin n\mu}{\sin \mu} .$$

6. The conjugate of the even function of  $\theta$  whose value for  $0 < \theta < \pi$  is

$$\log \left| \frac{\cos \frac{\theta}{2}}{\cos \left( \frac{\theta}{2} - \alpha \right)} \right| \text{ is given by}$$

$$G(\theta) = -\frac{\sin \theta}{\pi} \int_0^\pi \frac{\log \left| \frac{\cos \frac{\phi}{2}}{\cos \left( \frac{\phi}{2} - \alpha \right)} \right|}{\cos \theta - \cos \phi} d\phi .$$

Write  $t = \tan \frac{1}{2}\theta$ ,  $\phi = \tan \frac{1}{2}\phi$ ,  $\alpha = \cot \alpha$ .

Then since

$$\int_0^\pi \frac{\log \sin \alpha}{\cos \theta - \cos \phi} d\phi = 0,$$

$$\begin{aligned} G &= \frac{2t}{\pi} \int_0^\infty \frac{\log |a + p|}{p^2 - t^2} dp, \quad \text{as in section 3,} \\ &= \frac{2T}{\pi} \int_0^\infty \frac{\log |1 + P|}{P^2 - T^2} dP, \quad \text{where } P = \frac{p}{a}, \quad T = \frac{t}{a}, \\ &= \frac{1}{\pi} \int_0^\infty \frac{1}{1+P} \log \left| \frac{P+T}{P-T} \right| dP, \quad \text{integrating by parts.} \end{aligned}$$

$$\begin{aligned} \frac{dG}{dT} &= \frac{1}{\pi} \int_0^\infty \frac{1}{1+P} \left\{ \frac{1}{P+T} + \frac{1}{P-T} \right\} dP \\ &= \frac{2}{\pi} \frac{\log T}{T^2 - 1}. \end{aligned}$$

$G$  is an odd function of  $\theta$ , hence  $G(0) = 0$ .

Therefore

$$\begin{aligned} G &= \frac{2}{\pi} \int_0^T \frac{\log x}{x^2 - 1} dx \\ &= F(T). \end{aligned}$$

This is tabulated in Table 1.

$$\begin{aligned} A &= 2 \int_0^\pi \log \left| \frac{\cos \frac{\theta}{2}}{\cos \left( \frac{\theta}{2} - \alpha \right)} \right| d\theta \\ &= 2 \int_0^a \log \tan \frac{\theta}{2} d\theta \\ &= 4 \int_0^{\tan a} \frac{\log x}{1+x^2} dx. \end{aligned}$$

This form is useful when  $\tan \alpha$  is given exactly, as the integrand may be expanded in series, to give

$$A = -4 \left\{ \log \cot \alpha \left( \tan \alpha - \frac{\tan^3 \alpha}{3} + \frac{\tan^5 \alpha}{5} - \dots \right) + \left( \tan \alpha - \frac{\tan^3 \alpha}{9} + \frac{\tan^5 \alpha}{25} - \dots \right) \right\}.$$

If  $\alpha$  is an integral number of half-degrees, it is more convenient to use

$$\begin{aligned} A &= 2 \int_0^\pi \log \sin \frac{\theta}{2} d\theta - 2 \int_{2a}^{\pi+2a} \log \sin \frac{\theta}{2} d\theta, \\ &= -2\pi \{X(\pi) - X(\pi + 2\alpha) + X(2\alpha)\}, \\ &= -2\pi \{X(2\alpha) + X(\pi - 2\alpha) - X(\pi)\}. \end{aligned}$$

### APPENDIX III

#### *The Leading-Edge Term*

$$K = \frac{1}{2n} \cot \alpha_0 \left\{ |n\phi| + \cos n\phi - \frac{\pi}{2} \right\}, \quad -\frac{\pi}{2n} < \phi < \frac{\pi}{2n} \quad \dots \quad \dots \quad (\text{III.1})$$

This being an even function of  $\phi$ , the conjugate is

$$L = -\frac{\cot \alpha_0 \sin \phi}{2\pi n} \int_0^{\pi/2n} \frac{nt + \cos nt - \frac{\pi}{2}}{\cos \phi - \cos t} dt. \quad \dots \quad \dots \quad (\text{III.2})$$

$$\sin \phi \int_0^{\pi/2n} \frac{nt - \frac{\pi}{2}}{\cos \phi - \cos t} dt = -n \int_0^{\pi/2n} \log \left| \frac{\sin \frac{1}{2}(t - \phi)}{\sin \frac{1}{2}(t + \phi)} \right| dt.$$

The contribution of these terms to  $L$  is thus

$$\frac{\cot \alpha_0}{2\pi} \int_0^{\pi/2n} \log \left| \frac{\sin \frac{1}{2}(t - \phi)}{\sin \frac{1}{2}(t + \phi)} \right| dt. \quad \dots \quad \dots \quad \dots \quad (\text{III.3})$$

By Lemma 4 of Ref. 2, the value of the remaining term is

$$-\frac{\cot \alpha_0}{2\pi n} \left[ \cos n\phi \log \left| \frac{\sin \frac{1}{2}\left(\phi - \frac{\pi}{2n}\right)}{\sin \frac{1}{2}\left(\phi + \frac{\pi}{2n}\right)} \right| - \frac{\pi}{2n} \sin n\phi - 2 \sum_{s=0}^{n-2} \frac{\sin \frac{n-s-1}{2n}\pi}{n-s-1} \sin(s+1)\phi \right]. \quad (\text{III.4})$$

For a positive radius of curvature at  $\phi = 0$ ,  $d\chi/d\phi$  must be positive at  $\phi = 0$ .

The contribution of equation (III.3) to  $dL/d\phi$  is

$$\begin{aligned} & -\frac{\cot \alpha_0}{2\pi} \int_0^{\pi/2n} \left\{ \frac{1}{2} \cot \frac{1}{2}(t - \phi) + \frac{1}{2} \cot \frac{1}{2}(t + \phi) \right\} dt \\ & = -\frac{\cot \alpha_0}{2\pi} \left\{ \log \left| \sin \frac{1}{2}\left(\frac{\pi}{2n} - \phi\right) \right| + \log \left| \sin \frac{1}{2}\left(\frac{\pi}{2n} + \phi\right) \right| - 2 \log \sin \frac{1}{2}\phi \right\} \\ & \rightarrow \frac{\cot \alpha_0}{\pi} \left\{ \log \frac{\phi}{2} - \log \sin \frac{\pi}{4n} \right\} \text{ as } \phi \rightarrow 0. \quad \dots \quad \dots \quad \dots \quad (\text{III.5}) \end{aligned}$$

The contribution of equation (III.4) to  $dL/d\phi$  is

$$\begin{aligned} & \frac{\cot \alpha_0}{2\pi n} \left\{ n \sin n\phi \log \left| \frac{\sin \frac{1}{2}\left(\phi - \frac{\pi}{2n}\right)}{\sin \frac{1}{2}\left(\phi + \frac{\pi}{2n}\right)} \right| - \cos n\phi \left[ \frac{1}{2} \cot \frac{1}{2}\left(\phi - \frac{\pi}{2n}\right) - \frac{1}{2} \cot \frac{1}{2}\left(\phi + \frac{\pi}{2n}\right) \right] \right. \\ & \left. + \frac{\pi}{2} \cos n\phi + 2 \sum_{s=0}^{n-2} \frac{s+1}{n-s-1} \sin \frac{n-s-1}{2n}\pi \cdot \cos(s+1)\pi \right\} \\ & \rightarrow \frac{\cot \alpha_0}{2\pi n} \cdot \left\{ \cot \frac{\pi}{4n} + \frac{\pi}{2} + 2 \sum_{s=0}^{n-2} \frac{s+1}{n-s-1} \sin \frac{n-s-1}{2n}\pi \right\} \text{ as } \phi \rightarrow 0. \quad \dots \quad (\text{III.6}) \end{aligned}$$

The other main contribution to  $\chi$  in this region is due to the incidence term, and is

$$F \left\{ \tan \alpha_0 \tan \frac{1}{2}(\phi + \pi) \right\}.$$

For  $\phi$  small this is

$$\frac{\pi}{2} + \frac{2}{\pi} \int_0^{\cot a_0 \tan \frac{1}{2}\phi} \frac{\log x}{x^2 - 1} dx. \quad \dots \quad \dots \quad \dots \quad \dots \quad (\text{III.7})$$

The contribution to  $d\chi/d\phi$  is

$$\rightarrow -\frac{\cot \alpha_0}{\pi} \left( \log \cot \alpha_0 + \log \frac{\phi}{2} \right) \text{ as } \phi \rightarrow 0 . \quad \dots \quad \dots \quad \dots \quad \dots \quad (\text{III.8})$$

Combining equations (III.5), (III.6) and (III.8) a measure of  $d\chi/d\phi$  near  $\phi = 0$  is

$$-\frac{\cot \alpha_0}{\pi} \log \sin \frac{\pi}{4n} - \frac{\cot \alpha_0}{\pi} \log \cot \alpha_0 \\ + \frac{\cot \alpha_0}{2\pi n} \left( \cot \frac{\pi}{4n} + \frac{\pi}{2} + 2 \sum_{s=0}^{n-2} \frac{s+1}{n-s-1} \sin \frac{n-s-1}{2n} \pi \right).$$

The condition  $d\chi/d\phi > 0$  is thus

$$\frac{1}{2n} \left\{ \cot \frac{\pi}{4n} + \frac{\pi}{2} + 2 \sum_{s=0}^{n-2} \frac{s+1}{n-s-1} \sin \frac{n-s-1}{2n} \pi \right\} - \log \sin \frac{\pi}{4n} > \log \cot \alpha_0. \dots \quad (\text{III.9})$$

It is seen that the left-hand side is a function of  $n$  only, while the right-hand side is a function of  $\alpha_0$  only. Calculation gives

<i>n</i>	Left-hand side	$\alpha_0$ (deg)	Right-hand side
2	1·810	1	4·048
3	2·714	2	3·355
4	2·999	4	2·660
6	3·404	8	1·962
9	3·814	12	1·549

$n = 3$  may be used for  $\alpha_0 \geq 4$  deg,  $n = 6$  is sufficient for  $\alpha_0 \geq 2$  deg.

$2\alpha_0$  is the extent of the incidence range. Thus  $n = 6$  may be used if the incidence range extends over at least 4 deg.

$$K_6 = \frac{1}{12} \cot \alpha_0 \left( \left| 6\phi \right| + \cos 6\phi - \frac{\pi}{2} \right) - \frac{\pi}{12} < \phi < \frac{\pi}{12}. \quad \dots \quad \dots \quad (\text{III.10})$$

The conjugate  $L_6$  is the sum of equations (III.3) and (III.4), with  $n = 6$ .

The following relations are easily derived.

$$\left. \begin{aligned} \int K_6 d\phi &= \cot \alpha_0 \cdot \frac{1}{36} \left( 1 - \frac{\pi^2}{8} \right) \\ &= -0.006491682 \cot \alpha_0 \\ \int K_6 \cos \phi d\phi &= \cot \alpha_0 \left( \frac{36}{35} \cos \frac{\pi}{12} - 1 \right) \\ &= -0.006476320 \cot \alpha_0 \\ \int K_6 \sin \phi d\phi &= 0 \\ \int K_6 \cos 2\phi d\phi &= \cot \alpha_0 \left( \frac{9}{32} \sin \frac{\pi}{3} - \frac{1}{4} \right) \\ &= -0.006430356 \cot \alpha_0 \\ \int K_6 \sin 2\phi d\phi &= 0 \end{aligned} \right\} \quad \dots \quad \dots \quad \dots \quad \text{(III.11)}$$

In each case the integral is over the complete range  $[-\pi/12, \pi/12]$ .

In R. & M. 2112<sup>1</sup> a different leading-edge term is given, namely

$$K_0 = \frac{1}{2n} \cot \alpha_0 \{ |\sin n\phi| - 1 \}, \quad -\frac{\pi}{2n} < \phi < \frac{\pi}{2n}. \quad \dots \quad \dots \quad \text{(III.12)}$$

At  $\phi = 0$

$$K_0 = -\frac{1}{2n} \cot \alpha_0$$

At  $\phi = \frac{\pi}{2n}$

$$K_0 = 0$$

$$\frac{dK_0}{d\phi} = \pm \frac{1}{2} \cot \alpha_0$$

$$\frac{dK_0}{d\phi} = 0$$

$$\frac{d^2K_0}{d\phi^2} = 0.$$

$$\frac{d^2K_0}{d\phi^2} = -\frac{n}{2} \cot \alpha_0.$$

The discontinuity is eliminated, but analysis shows that a very large value of  $n$  is necessary to get a positive radius of curvature at  $\phi = 0$ . The conjugate function is troublesome, and asymptotic formulae have to be used. Another disadvantage is the large discontinuity in  $d^2K_0/d\phi^2$  at  $\phi = \pm \pi/2n$ . Both  $n$  and  $\cot \alpha_0$  are large, so the shape may be a little awkward in the neighbourhood.

The term given in equation (43) is

$$K = \frac{1}{2n} \cot \alpha_0 \left\{ \left| n\phi \right| + \cos n\phi - \frac{\pi}{2} \right\}, \quad -\frac{\pi}{2n} < \phi < \frac{\pi}{2n}.$$

$$\begin{aligned}
\text{At } \phi = 0 \quad K &= -\frac{\pi - 2}{4n} \cot \alpha_0 & \text{At } \phi = \pm \frac{\pi}{2n} \quad K &= 0 \\
\frac{dK}{d\phi} &= \pm \frac{1}{2} \cot \alpha_0 & \frac{dK}{d\phi} &= 0 \\
\frac{d^2K}{d\phi^2} &= -\frac{n}{2} \cot \alpha_0. & \frac{d^2K}{d\phi^2} &= 0.
\end{aligned}$$

The maximum value of  $d^2K/d\phi^2$  is now at  $\phi = 0$ , and there is no discontinuity of  $d^2K/d\phi^2$  anywhere. As shown above, quite small values of  $n$  may be used, and it is a practicable proposition to tabulate the conjugate exactly.

---

## APPENDIX IV

### *Design of an Aerofoil*

A suction aerofoil is required with a slot at about 70 per cent chord on the upper surface, an incidence range extending from  $\alpha = 0$  to as high a value as possible, and a thickness of about 30 per cent of the chord. This type of section would probably be used in an all-wing aeroplane, so it is also required that  $C_{M0} = 0$ . On the lower surface the velocity is to be increasing back to about 60 per cent chord, to secure a large extent of laminar flow. Thereafter on the chord the velocity is to fall steadily, at a rate which, it is hoped, will not produce separation.

The velocity distribution selected is

$$\log q_0 = \left\{ \begin{array}{lll} \log \left| \frac{\cos \frac{\theta}{2}}{\cos (\frac{\theta}{2} - \alpha)} \right| & , & \alpha < \theta < \pi + \alpha \\ + l & , & 0 < \theta < 2\pi \\ + m & , & \beta < \theta < \pi + \alpha - \varepsilon \\ + (\pi + \alpha - \theta) \cot \frac{1}{2}\alpha & , & \pi + \alpha - \varepsilon < \theta < \pi + \alpha \\ - j(\cos \theta - \cos \delta) & , & 2\pi - \delta < \theta < 2\pi \\ - j(1 - \cos \delta) - k & , & 0 < \theta < \beta \\ + \frac{1}{2}kP_6(\theta) & , & [\text{the trailing-edge term}] \end{array} \right. . \quad (\text{IV.1})$$

Here the range of  $\theta$  is specified over which each term applies. From the design conditions, choose  $\alpha = 15$  deg,  $\beta = 50$  deg,  $\delta = 70$  deg. Behind the slot the distance is greater than is indicated by the rule  $x \simeq \frac{1}{2}(1 - \cos \theta)$ , since the velocity is low and  $ds/d(\cos \theta)$  is proportional to  $1/q_0$ , by equation (9). When this section was designed the leading-edge term was still under

development, but it was considered that for an aerofoil of this thickness, the logarithmically infinite curvature at  $\theta = \pi + \alpha - \varepsilon$  would not be important. The four parameters  $l, m, j$  and  $k$  are left arbitrary to enable equation (23)  $A, B$  and  $C$ , and also equation (28) to be satisfied.

For satisfying equation (23)  $B$  and  $C$ , it is convenient to consider instead the equivalent equations

$$\int_{-\pi}^{\pi} \log q_0 \cos(\theta - \alpha) d\theta = 0$$

and

$$\int_{-\pi}^{\pi} \log q_0 \sin(\theta - \alpha) d\theta = 0.$$

Call these equations  $B'$  and  $C'$  respectively. All the expressions occurring in equation (IV.1) are given in Appendix I.

$$\text{From continuity of } \log q_0 \text{ at } \theta = \pi + \alpha - \varepsilon, \quad \varepsilon = m \tan \frac{1}{2}\alpha. \quad \dots \quad \dots \quad \dots \quad (\text{IV.2})$$

$\varepsilon$  must be found by a process of successive approximation, as explained in section 3.  $B', C'$  and equation (28) are first solved with  $\varepsilon = 0$ .

$$\begin{aligned} B' &= 2 \sin 15^\circ \log \cot 7\frac{1}{2}^\circ - m \sin 35^\circ - \frac{1}{4}j \{-\sin 15^\circ + \sin 25^\circ + \frac{7}{9}\pi \cos 15^\circ\} \\ &\quad + j \cos 70^\circ \{\sin 85^\circ - \sin 15^\circ\} - j(1 - \cos 70^\circ) \{\sin 15^\circ + \sin 35^\circ\} \\ &\quad - k \{\sin 15^\circ + \sin 35^\circ\} + 0.0064763k \sin 15^\circ + B_m' = 0, \\ &\quad - 0.573576m - 0.830719k - 0.926502j + 1.049556 + B_m' = 0. \quad \dots \quad (\text{IV.3}) \end{aligned}$$

$$\begin{aligned} C' &= \pi \sin 15^\circ + m \{\cos 35^\circ + 1\} + \frac{1}{4}j \{\cos 15^\circ + \cos 25^\circ + \frac{7}{9}\pi \sin 15^\circ\} \\ &\quad + j \cos 70^\circ \{\cos 85^\circ - \cos 15^\circ\} - j(1 - \cos 70^\circ) \{\cos 15^\circ - \cos 35^\circ\} \\ &\quad - k \{\cos 15^\circ - \cos 35^\circ\} + 0.0064763k \cos 15^\circ + C_m' = 0, \\ &\quad 1.819152m - 0.140518k + 0.229031j - 0.813103 + C_m' = 0. \quad \dots \quad (\text{IV.4}) \end{aligned}$$

$$\begin{aligned} (28) &= 2 \sin 15^\circ \sin 30^\circ + \frac{1}{4}\pi \sin 60^\circ - \sin^2 30^\circ \log \cot 7\frac{1}{2}^\circ \\ &\quad + \frac{1}{2}m \{\cos 100^\circ - \cos 30^\circ\} - \frac{1}{6}j \{-\cos 30^\circ + 3 \cos 70^\circ - 4\} \\ &\quad + \frac{1}{2}j \cos 70^\circ \{-\cos 40^\circ - 1\} - \frac{1}{2}j(1 - \cos 70^\circ) \{1 + \cos 80^\circ\} \\ &\quad - \frac{1}{2}k \{1 + \cos 80^\circ\} + 0.0128607k + M_m' = 0 \\ &\quad - 0.519837m - 0.573963k - 0.048136j + 0.432096 + M_m' = 0. \quad \dots \quad (\text{IV.5}) \end{aligned}$$

$B_m', C_m', M_m'$  represent the extra terms when  $\varepsilon = m \tan \frac{1}{2}\alpha$ .

From Appendix I,

$$\begin{aligned} B_m' &= \cot \frac{1}{2}\alpha \{1 - \cos(m \tan \frac{1}{2}\alpha)\} \\ &= 7.595754 \{1 - \cos(7.54313^\circ m)\}. \quad \dots \quad \dots \quad \dots \quad \dots \quad \dots \quad (\text{IV.6}) \end{aligned}$$

$$\begin{aligned} C_m' &= -m + \cot \frac{1}{2}\alpha \sin(M \tan \frac{1}{2}\alpha) \\ &= -m + 7.595754 \sin(7.54313^\circ m) \dots \dots \dots \dots \dots \quad (IV.7) \end{aligned}$$

$$\begin{aligned} M_m' &= \frac{1}{2}m \cos 2\alpha - \frac{1}{2} \cot \frac{1}{2}\alpha \cos(2\alpha - m \tan \frac{1}{2}\alpha) \sin(m \tan \frac{1}{2}\alpha) \\ &= 0.433013m - 3.797877 \cos(30^\circ - 7.54313^\circ m) \sin(7.54313^\circ m) \dots \quad (IV.8) \end{aligned}$$

Elimination of  $j$  and  $k$  from equations (IV.3), (IV.4) and (IV.5) gives

$$0.981944m + 0.138219B_m' + 0.491790C_m' - 0.320451M_m' - 0.393273 = 0 \dots \quad (IV.9)$$

With  $B_m' = C_m' = M_m' = 0$ , this gives  $m = 0.400504$ .

Hence from equations (IV.6), (IV.7), (IV.8),

$$B_m' = 0.010556, C_m' = -0.000187, M_m' = -0.004953.$$

With these values, (IV.9) gives  $m = 0.397496$ .

Hence  $B_m' = 0.010399, C_m' = -0.000181, M_m' = -0.004822$ .

With these values, (IV.9) gives  $m = 0.397541$ .

Hence  $B_m' = 0.010419, C_m' = -0.000182, M_m' = -0.004822$ .

With these values, (IV.9) gives  $m = 0.397536$ .

Hence  $B_m' = 0.010419, C_m' = -0.000181, M_m' = -0.004822$ .

With these values, equation (IV.9) gives  $m = 0.397536$ .

The final result is thus

$$\begin{aligned} m &= 0.397536, \\ \varepsilon &= 2^\circ 59.920', \quad = 2.99866^\circ. \end{aligned}$$

From equations (IV.3), (IV.4), (IV.5) it now follows that

$$\begin{aligned} j &= 0.598405, \\ k &= 0.334090. \end{aligned}$$

Equation (23)A, multiplied by  $180/\pi$ , gives

$$\begin{aligned} &-360 \{X(15^\circ) + X(165^\circ) - X(180^\circ)\} + 360l + (180 + 15 - \varepsilon - 50)m + \frac{1}{2}\varepsilon m \\ &- \frac{180}{\pi}j \sin 70^\circ + 70j \cos 70^\circ - 50j(1 - \cos 70^\circ) - 50k = 0, \dots \dots \quad (IV.10) \end{aligned}$$

from which

$$l = 0.244941.$$

The velocity distribution is now completely determined. Inspection shows that the values obtained for the parameters indicate that the aerofoil is likely to be satisfactory.

From Appendix I, the conjugate of  $\log q_0$  is easily written down as

Substituting the known values, and arranging in a form suitable for computation, this becomes, in degrees,

$$\begin{aligned} \chi = & F \left\{ 0.1316525 \tan \frac{1}{2}(\theta - 15^\circ) \right\} + 0.167045 Q_6(\theta) - 6.6667 \sin \theta \\ & + (25.1295 \cos \theta - 8.5948) \log_{10} |\cosec \frac{1}{2}(\theta + 70^\circ)| \\ & + (-25.1295 \cos \theta + 39.1593) \log_{10} |\cosec \frac{1}{2}\theta| \\ & - 47.2587 \log_{10} |\cosec \frac{1}{2}(\theta - 50^\circ)| \\ & + 435.2047 \{ X(\theta - 192.00134^\circ) - X(\theta - 195^\circ) \}. \quad \dots \quad \dots \quad (\text{IV.12}) \end{aligned}$$

The next step is to select the values of  $\theta$  at which the integrals of equation (11) are to be calculated, to enable the aerofoil shape to be found by numerical integration. The interval of tabulation is reduced near the leading edge and near the discontinuity. In the latter region a still closer spacing than that actually chosen might have been desirable. In Table 7, the results of the computation, carried out using seven-figure tables, are shown.  $\chi$  is tabulated, and then the integrands of equation (11). For convenience the constant factor  $2/e^l$  is omitted. The integration is now performed by Simpson's rule, assisted as necessary by the cubic rule as explained in section 7, from the trailing edge round the surface in each direction to the slot, to get the aerofoil co-ordinates  $x$  and  $y$ . Logarithmic spiral theory shows that the aerofoil contour closes up satisfactorily and enables the slot position itself to be determined.

The chord length is measured and found to be 71.275 in these co-ordinates. Allowing for the factor  $2/e^l$  and for the fact that 5 deg was taken as the unit in performing the integrations, the true chord length is calculated to be 3.2458. In Table 7, the aerofoil contour is given in co-ordinates  $X$  and  $Y$ , in which the chord is of unit length and lies along the  $X$ -axis, and finally the surface velocity is tabulated at the bottom and top of the incidence range.

The properties of the aerofoil can now be calculated.

The lift coefficient at the top of the incidence range is

$$C_L = \frac{8\pi \sin \alpha}{c}$$

$$= 2 \cdot 004.$$

The lift-curve slope

$$= \frac{8\pi}{c} = 7.743.$$

In the  $(x,y)$  co-ordinates the aerofoil would be at the no-lift angle, if no constants had been omitted from  $\chi$ . By Appendix I, the omitted terms are

$$\begin{aligned} & \frac{1}{2}\alpha + \frac{1}{2\pi} j(1 - \cos \delta) \\ & = 11^\circ 5\frac{1}{2}' . \end{aligned}$$

Thus in the  $(x,y)$  co-ordinates, the no-lift angle is  $-11^\circ 5\frac{1}{2}'$  min. To get the chord line horizontal in the  $(X,Y)$  co-ordinates, a rotation of  $9^\circ 16\frac{1}{2}'$  min was imposed. Hence, relative to the chord line, the no-lift angle is  $-1^\circ 49$  min.

By use of equations (29) and (31) the aerodynamic centre of the aerofoil is found to be at  $X = 0.3077$ .

The thickness of the section is 31.5 per cent and the position of the suction slot is  $X = 0.6911$ . The whole design fulfils satisfactorily the requirements of the initial specification. The aerofoil is shown in Fig. 2.

---

## REFERENCES

No.	Author			Title, etc.
1	M. J. Lighthill	..	..	A new method of two-dimensional aerodynamic design. R. & M. 2112. April, 1945.
2	S. Goldstein	..	..	A theory of aerofoils of small thickness. Part II. Velocity distributions for cambered aerofoils. A.R.C. 6156. (To be published).
3	M. J. Lighthill	..	..	A theoretical discussion of wings with leading edge suction. R. & M. 2162. May, 1945.
4	M. B. Glauert	..	..	The design of suction aerofoils with a very large $C_L$ -range. R. & M. 2111. November, 1945.

---

TABLE 1

$T$	$F(T)$	$\Delta$	$-\Delta^2$	$T$	$F(T)$	$\Delta$	$-\Delta^2$	$T$	$F(T)$	$\Delta$	$-\Delta^2$
0	0	52632		0.092	11.38836	17478	154	0.182	18.10116	12819	73
0.002	0.52632	42518		0.094	11.56314	17328	150	0.184	18.22935	12746	73
0.004	0.95150	38702		0.096	11.73642	17182	146	0.186	18.35681	12674	72
0.006	1.33852	36224		0.098	11.90824	17039	143	0.188	18.48355	12604	70
0.008	1.70076	34382		0.100	12.07863	16897	142	0.190	18.60959	12534	70
0.010	2.04458	32914									
0.012	2.37372	31694		0.102	12.24760	16760	137	0.192	18.73493	12466	68
0.014	2.69066	30650		0.104	12.41520	16625	135	0.194	18.85959	12398	68
0.016	2.99716	29737		0.106	12.58145	16493	132	0.196	18.98357	12329	69
0.018	3.29453	28926		0.108	12.74638	16363	130	0.198	19.10686	12263	66
0.020	3.58379	28197	729	0.110	12.91001	16237	126	0.200	19.27949	12204	66
0.022	3.86576	27535	662	0.112	13.07238	16112	125				
0.024	4.14111	26929	606	0.114	13.23350	15989	123	0.200	19.22949	30372	410
0.026	4.41040	26371	558	0.116	13.39339	15870	119	0.205	19.53321	29972	400
0.028	4.67411	25852	519	0.118	13.55209	15752	118	0.210	19.83293	29584	388
0.030	4.93263	25367	485	0.120	13.70961	15636	116	0.215	20.12877	29204	380
0.032	5.18630	24914	453	0.122	13.86597	15521	115	0.220	20.42081	28836	368
0.034	5.43544	24487	427	0.124	14.02118	15410	111	0.225	20.70917	28478	358
0.036	5.68031	24085	402	0.126	14.17528	15301	109	0.230	20.99395	28127	351
0.038	5.92116	23704	381	0.128	14.32829	15194	107	0.235	21.27522	27787	340
0.040	6.15820	23342	362	0.130	14.48023	15086	108	0.240	21.55309	27453	334
0.042	6.39162	22998	344	0.132	14.63109	14982	106	0.245	21.82762	27127	326
0.044	6.62160	22669	329	0.134	14.78091	14880	102	0.250	22.09889	26810	317
0.046	6.84829	22356	313	0.136	14.92971	14779	101	0.255	22.36699	26500	310
0.048	7.07185	22055	301	0.138	15.07750	14679	99	0.260	22.63199	26198	302
0.050	7.29240	21767	288	0.140	15.22429	14580	99	0.265	22.89397	25903	295
0.052	7.51007	21490	277	0.142	15.37009	14486	94	0.270	23.15300	25614	289
0.054	7.72497	21225	265	0.144	15.51495	14389	97	0.275	23.40914	25331	283
0.056	7.93722	20967	258	0.146	15.65884	14296	93	0.280	23.66245	25053	278
0.058	8.14689	20719	248	0.148	15.80180	14204	92	0.285	23.91298	24782	271
0.060	8.35408	20480	239	0.150	15.94384	14113	91	0.290	24.16080	24518	264
0.062	8.55888	20249	231	0.152	16.08497	14023	90	0.295	24.40598	24257	261
0.064	8.76137	20024	225	0.154	16.22520	13936	87	0.300	24.64855	24003	254
0.066	8.96161	19808	216	0.156	16.36456	13849	87	0.305	24.88858	23754	249
0.068	9.15969	19598	210	0.158	16.50305	13763	86	0.310	25.12612	23510	244
0.070	9.35567	19395	203	0.160	16.64068	13677	86	0.315	25.36122	23271	239
0.072	9.54962	19195	200	0.162	16.77745	13595	82	0.320	25.59393	23036	235
0.074	9.74157	19003	192	0.164	16.91340	13513	82	0.325	25.82429	22804	232
0.076	9.93160	18817	186	0.166	17.04853	13430	83	0.330	26.05233	22578	226
0.078	10.11977	18635	182	0.168	17.18283	13350	80	0.335	26.27811	22357	221
0.080	10.30612	18456	179	0.170	17.31633	13273	77	0.340	26.50168	22139	218
0.082	10.49068	18282	174	0.172	17.44906	13194	79	0.345	26.72307	21925	214
0.084	10.67350	18114	168	0.174	17.58100	13117	77	0.350	26.94232	21714	211
0.086	10.85464	17950	164	0.176	17.71217	13041	76	0.355	27.15946	21510	204
0.088	11.03414	17790	160	0.178	17.84258	12966	75	0.360	27.37456	21308	202
0.090	11.21204	17632	158	0.180	17.97224	12892	74	0.365	27.58764	21107	201
0.092	11.38836		154	0.182	18.10116		73	0.370	27.79871	20913	194
								0.375	28.00784	20719	194
								0.380	28.21503		188

TABLE 1—*continued*

$T$	$F(T)$	$\Delta$	$-\Delta^2$	$T$	$F(T)$	$\Delta$	$-\Delta^2$	$T$	$F(T)$	$\Delta$	$-\Delta^2$
0.380	28.21503	20531	188	0.50	32.68504	33451	525	0.76	40.01580	23558	286
0.385	28.42034	20347	184	0.51	33.01955	32943	508	0.77	40.25138	23277	281
0.390	28.62381	20163	184	0.52	33.34898	32449	494	0.78	40.48415	23005	272
0.395	28.82544	19982	181	0.53	33.67347	31965	484	0.79	40.71420	22739	266
0.400	29.02526	19807	175	0.54	33.99312	31494	471	0.80	40.94159	22479	260
0.405	29.22333	19633	174	0.55	34.30806	31037	457				
0.410	29.41966	19462	171	0.56	34.61843	30591	446	0.81	41.16638	22224	255
0.415	29.61428	19293	169	0.57	34.92434	30156	435	0.82	41.38862	21971	253
0.420	29.80721	19126	167	0.58	35.22590	29732	424	0.83	41.60833	21723	248
0.425	29.99847	18964	162	0.59	35.52322	29316	416	0.84	41.82556	21480	243
0.430	30.18811	18804	160	0.60	35.81638	28912	404	0.85	42.04036	21241	239
0.435	30.37615	18645	159		36.10550	28517	395	0.86	42.25277	21008	233
0.440	30.56260	18490	155	0.61	36.39067	28132	385	0.87	42.46285	20782	226
0.445	30.74750	18337	153	0.62	36.67199	27758	374	0.88	42.67067	20557	225
0.450	30.93087	18186	151	0.63	36.94957	27392	366	0.89	42.87624	20334	223
0.455	31.11273	18038	148	0.64	37.22349	27031	361	0.90	43.07958	20119	215
0.460	31.29311	17891	147		37.49380	26679	352	0.91	43.28077	19909	210
0.465	31.47202	17747	144	0.66	37.76059	26337	342	0.92	43.47986	19699	210
0.470	31.64949	17604	143	0.67	38.02396	26003	334	0.93	43.67685	19494	205
0.475	31.82553	17463	141	0.68	38.28399	25671	322	0.94	43.87179	19292	202
0.480	32.00016	17324	139	0.69	38.54070	25346	325	0.95	44.06471	19091	201
0.485	32.17340	17188	136		38.79416	25032	314	0.96	44.25562	18893	198
0.490	32.34528	17054	134	0.71	39.04448	24727	305	0.97	44.44455	18703	190
0.495	32.51582	16922	132	0.72	39.29175	24428	299	0.98	44.63158	18515	188
0.500	32.68504		131	0.73	39.53603	24133	295	0.99	44.81673	18327	188
				0.74	39.77736	23844	289	1.00	45.00000		185
				0.75							
				0.76	40.01580	286					

*Notes on Table 1*

$$F(T) = \frac{360}{\pi^2} \int_0^T \frac{\log x}{x^2 - 1} dx.$$

It occurs in many of the conjugates in Appendix I, and is tabulated directly in degrees. It is the true conjugate multiplied by  $180/\pi$ .

Interpolation may be done by use of Bessel's formula, using the coefficients given in Table 6. The values should be accurate to 4 decimal places.

For  $T > 1$ , use  $F(T) = 90 - F\left(\frac{1}{T}\right)$

For  $T < 0$ , use  $F(-T) = -F(T)$

For  $T < 0.02$ , interpolation is inaccurate. Use the relation

$$F(T) = 83.988 \left\{ (T + \frac{1}{3}T^3) \log_{10} \frac{1}{T} + 0.43429 (T + \frac{1}{9}T^3) \right\}.$$

The terms of higher order are negligible.

The relation  $\int_0^\infty \frac{\log x}{x^2 - 1} dx = \frac{\pi^2}{4}$  may be shown directly by contour integration.

TABLE 2

$\theta$ deg	$X(\theta)$	$\Delta$ +	$\Delta^2$ —	$\theta$ deg	$X(\theta)$	$\Delta$ +	$\Delta^2$ —	$\theta$ deg	$X(\theta)$	$\Delta$ +	$\Delta^2$ —
0	0										
1	0.0318965	318965	77014	46	0.4911047	51641	1142	91	0.6400358	18537	476
2	0.0560916	241951	29067	47	0.4962688	50526	1115	92	0.6418895	18068	469
3	0.0773800	212884	18874	48	0.5013214	49437	1089	93	0.6436963	17608	460
4	0.0967810	194010	14031	49	0.5062651	48373	1064	94	0.6454571	17157	451
5	0.1147789	179979	11179	50	0.5111024	47333	1040	95	0.6471728	16711	446
6	0.1316589	159505	9295	51	0.5158357	46317	1016	96	0.6488439	16277	434
7	0.1476094	7953	52	0.5204674	45323	994	97	0.6504716	15845	432	
8	0.1627646	151552	6952	53	0.5249997	44350	973	98	0.6520561	15426	419
9	0.1772246	144600	6173	54	0.5294347	43399	951	99	0.6535987	15010	416
10	0.1910673	138427	5550	55	0.5337746	42467	932	100	0.6550997	14605	405
11	0.2043550	127835	5042	56	0.5380213	41556	911	101	0.6565602	14205	400
12	0.2171385	4619	57	0.5421769	40663	893	102	0.6579807	13811	394	
13	0.2294601	123216	4259	58	0.5462432	39787	876	103	0.6593618	13427	384
14	0.2413558	118957	3952	59	0.5502219	38931	856	104	0.6607045	13047	380
15	0.2528563	115005	3685	60	0.5541150	38091	840	105	0.6620092	12676	371
16	0.2639883	107869	3451	61	0.5579241	37269	822	106	0.6632768	12310	366
17	0.2747752	3247	62	0.5616510	36460	809	107	0.6645078	11952	358	
18	0.2852374	104622	3062	63	0.5652970	35670	790	108	0.6657030	11599	353
19	0.2953934	101560	2899	64	0.5688640	34894	776	109	0.6668629	11253	346
20	0.3052595	98661	2751	65	0.5723534	34133	761	110	0.6679882	10914	339
21	0.3148505	93294	2616	66	0.5757667	33387	746	111	0.6690796	10580	334
22	0.3241799	2495	67	0.5791054	32653	734	112	0.6701376	10254	326	
23	0.3332598	90799	2384	68	0.5823707	31936	717	113	0.6711630	9933	321
24	0.3421013	88415	2282	69	0.5855643	31230	706	114	0.6721563	9617	316
25	0.3507146	86133	2187	70	0.5886873	30537	693	115	0.6731180	9309	308
26	0.3591092	81845	2101	71	0.5917410	29857	680	116	0.6740489	9006	303
27	0.3672937	2019	72	0.5947267	29191	666	117	0.6749495	8709	297	
28	0.3752763	79826	1945	73	0.5976458	28535	656	118	0.6758204	8418	291
29	0.3830644	77881	1875	74	0.6004993	27891	644	119	0.6766622	8132	284
30	0.3906650	76006	1810	75	0.6032884	27260	631	120	0.6774754	7852	280
31	0.3980846	74196	1749	76	0.6060144	26639	621	121	0.6782606	7578	274
32	0.4053293	72447	1690	77	0.6086783	26030	609	122	0.6790184	7309	269
33	0.4124050	70757	1638	78	0.6112813	25431	599	123	0.6797493	7046	263
34	0.4193169	69119	1585	79	0.6138244	24843	588	124	0.6804539	6788	258
35	0.4260703	67534	1539	80	0.6163087	24265	578	125	0.6811327	6536	252
36	0.4326698	64504	1491	81	0.6187352	23698	567	126	0.6817863	6289	247
37	0.4391202	63054	1450	82	0.6211050	23139	559	127	0.6824152	6047	242
38	0.4454256	1408	83	0.6234189	22592	547	128	0.6830199	5810	237	
39	0.4515902	61646	1369	84	0.6256781	22054	538	129	0.6836009	5579	231
40	0.4576179	60277	1332	85	0.6278835	21523	531	130	0.6841588	5354	225
41	0.4635124	58945	1298	86	0.6300358	21004	519	131	0.6846942	5132	222
42	0.4692771	57647	1261	87	0.6321362	20493	511	132	0.6852074	4916	216
43	0.4749157	56386	1233	88	0.6341855	19992	501	133	0.6856990	4706	210
44	0.4804310	55153	1199	89	0.6361847	19498	494	134	0.6861696	4499	207
45	0.4858264	53954	1171	90	0.6381345	19013	485	135	0.6866195	4299	200
46	0.4911047	52783	1142	91	0.6400358	476	136	0.6870494	196		

TABLE 2—*continued*

$\theta$ deg	$X(\theta)$	$\Delta$ +	$\Delta^2$ —	$\theta$ deg	$X(\theta)$	$\Delta$ +	$\Delta^2$ —	$\theta$ deg	$X(\theta)$	$\Delta$ +	$\Delta^2$ —
136	0.6870494			196	151 0.6914163			166	0.6929534		59
137	0.6874597	4103		190	152 0.6915899	1736		126 167	0.6929921	387	56
138	0.6878510	3913		187	153 0.6917515	1616		117 168	0.6930252	331	51
139	0.6882236	3726		182	154 0.6919014	1499		112 169	0.6930532	280	46
140	0.6885780	3544		175	155 0.6920401	1387		107 170	0.6930766	234	43
		3369				1280				191	
141	0.6889149	3196		173	156 0.6921681	1177		103 171	0.6930957	154	37
142	0.6892345	3030		166	157 0.6922858	1078		99 172	0.6931111	119	35
143	0.6895375	2867		163	158 0.6923936			94 173	0.6931230	89	30
144	0.6898242	2710		157	159 0.6924920			91 174	0.6931319	65	24
145	0.6900952	2557		153	160 0.6925813			89 175	0.6931384	43	22
					809						
146	0.6903509	2409		148	161 0.6926622	727		82 176	0.6931427	26	17
147	0.6905918	2265		144	162 0.6927349			76 177	0.6931453	13	13
148	0.6908183	2126		139	163 0.6928000			651 73	0.6931466	5	8
149	0.6910309	1992		134	164 0.6928578			578 68	0.6931471	1	4
150	0.6912301	1862		130	165 0.6929088			510 64	0.6931472		0
151	0.6914163			126	166 0.6929534			446 59			

*Notes on Table 2*

$$X(\theta) = -\frac{1}{\pi} \int_0^\theta \log \sin \frac{1}{2}t dt.$$

Second differences are given to enable interpolation to be carried out by Bessel's formula, using Table 6.

For values of  $\theta$  outside the range given, use

$$X(180^\circ + \theta) = 2X(180^\circ) - X(180^\circ - \theta)$$

and

$$X(-\theta) = -X(\theta).$$

$X(180^\circ) = \log_e 2$ , as may be shown by integrating from 0 to  $\pi$ ,

$$\log \sin t = \log 2 + \log \sin \frac{1}{2}t + \log \cos \frac{1}{2}t.$$

To evaluate  $\{X(\alpha) + X(\pi - \alpha) - X(\pi)\}$  when  $\tan \alpha$  is known exactly, it is often convenient to make use of the series given in Appendix II, section 6.

TABLE 3

$\phi$ deg	$L_6'(\phi)$	$\Delta$	$\Delta^2$	$\phi$ deg	$L_6'(\phi)$	$\Delta$	$\Delta^2$	$\phi$ deg	$L_6'(\phi)$	$\Delta$	$\Delta^2$
0	0	82257	0	46	212·6633	22730	512	91	278·1040	8141	218
1	8·2257	81895	362	46	214·9363	22238	492	92	278·9181	7938	203
2	16·4152	81177	718	47	217·1601	21751	487	93	279·7119	7736	202
3	24·5329	80114	1063	48	219·3352	21282	469	94	280·4855	7545	191
4	32·5443	78718	1396	49	221·4634	20818	464	95	281·2400	7342	203
5	40·4161	77014	1704	50							
6	48·1175	75023	1991	51	223·5452	20370	448	96	281·9742	7153	189
7	55·6198	72779	2244	52	225·5822	19927	443	97	282·6895	6964	189
8	62·8977	70315	2464	53	227·5749	19499	428	98	283·3859	6787	177
9	69·9292	67671	2644	54	229·5248	19076	423	99	284·0646	6598	189
10	76·6963	64896	2775	55	231·4324	18667	409	100	284·7244	6422	176
11	83·1859	62038	2858	56	233·2991	18261	406	101	285·3666	6246	176
12	89·3897	59159	2879	57	235·1252	17870	391	102	285·9912	6080	166
13	95·3056	56333	2826	58	236·9122	17481	389	103	286·5992	5905	175
14	100·9389	53657	2676	59	238·6603	17106	375	104	287·1897	5741	164
15	106·3046	51323	2334	60	240·3709	16733	373	105	287·7638	5576	165
16	111·4369	49353	1970	61	242·0442	16372	361	106	288·3214	5424	152
17	116·3722	47599	1754	62	243·6814	16014	358	107	288·8638	5259	165
18	121·1321	45999	1600	63	245·2828	15668	346	108	289·3897	5107	152
19	125·7320	44525	1474	64	246·8496	15324	344	109	289·9004	4955	152
20	130·1845	43154	1371	65	248·3820	14992	332	110	290·3959	4813	142
21	134·4999	41869	1285	66	249·8812	14660	332	111	290·8772	4660	153
22	138·6868	40661	1208	67	251·3472	14341	319	112	291·3432	4519	141
23	142·7529	39519	1142	68	252·7813	14022	319	113	291·7951	4377	142
24	146·7048	38436	1083	69	254·1835	13714	308	114	292·2328	4246	131
25	150·5484	37405	1031	70	255·5549	13408	306	115	292·6574	4104	142
26	154·2889	36423	982	71	256·8957	13111	297	116	293·0678	3973	131
27	157·9312	35483	940	72	258·2068	12816	295	117	293·4651	3843	130
28	161·4795	34582	901	73	259·4884	12530	286	118	293·8494	3720	123
29	164·9377	33719	863	74	260·7414	12245	285	119	294·2214	3590	130
30	168·3096	32886	833	75	261·9659	11970	275	120	294·5804	3469	121
31	171·5982	32091	795	76	263·1629	11696	274	121	294·9273	3349	120
32	174·8073	31316	775	77	264·3325	11430	266	122	295·2622	3236	113
33	177·9389	30577	739	78	265·4755	11166	264	123	295·5858	3115	121
34	180·9966	29853	724	79	266·5921	10909	257	124	295·8973	3004	111
35	183·9819	29162	691	80	267·6830	10654	255	125	296·1977	2893	111
36	186·8981	28485	677	81	268·7484	10403	251	126	296·4870	2789	104
37	189·7466	27837	648	82	269·7887	10169	234	127	296·7659	2679	110
38	192·5303	27199	638	83	270·8056	9917	252	128	297·0338	2576	103
39	195·2502	26589	610	84	271·7973	9684	233	129	297·2914	2476	100
40	197·9091	25988	601	85	272·7657	9451	233	130	297·5390	2380	96
41	200·5079	25412	576	86	273·7108	9231	220	131	297·7770	2279	101
42	203·0491	24843	569	87	274·6339	8998	233	132	298·0049	2186	93
43	205·5334	24298	545	88	275·5337	8781	217	133	298·2235	2094	92
44	207·9632	23759	539	89	276·4118	8563	218	134	298·4329	2008	86
45	210·3391	23242	517	90	277·2681	8359	204	135	298·6337	1915	93
46	212·6633		512	91	278·1040	218	136	136	298·8252		84

TABLE 3—*continued*

$\phi$ deg	$L_6'(\phi)$	$\Delta$	$\frac{\Delta^2}{-}$	$\phi$ deg	$L_6'(\phi)$	$\Delta$	$\frac{\Delta^2}{-}$	$\phi$ deg	$L_6'(\phi)$	$\Delta$	$\frac{\Delta^2}{-}$
136	298.8252	1831	84	151	300.7913	796	59	166	301.5213	209	26
137	299.0083	1747	84	152	300.8709	744	52	167	301.5422	183	26
138	299.1830	1669	78	153	300.9453	694	50	168	301.5605	161	22
139	299.3499	1586	83	154	301.0147	647	47	169	301.5766	142	19
140	299.5085	1509	77	155	301.0794	597	50	170	301.5908	124	18
141	299.6594	1435	74	156	301.1391	552	45	171	301.6032	105	19
142	299.8029	1365	70	157	301.1943	510	42	172	301.6137	90	15
143	299.9394	1290	75	158	301.2453	471	39	173	301.6227	80	10
144	300.0684	1222	68	159	301.2924	428	43	174	301.6307	68	12
145	300.1906	1155	67	160	301.3352	392	36	175	301.6375	57	11
146	300.3061	1094	61	161	301.3744	357	35	176	301.6432	50	7
147	300.4155	1027	67	162	301.4101	325	32	177	301.6482	46	4
148	300.5182	967	60	163	301.4426	291	34	178	301.6528	42	4
149	300.6149	909	58	164	301.4717	261	30	179	301.6570	39	3
150	300.7058	855	54	165	301.4978	235	26	180	301.6609	0	
151	300.7913		59	166	301.5213		26				

*Notes on Table 3*

$L_6(\phi)$  is the conjugate of the leading-edge term, as developed in Appendix III, and is an odd function of  $\phi$ , where  $\phi = \theta - K$ ,  $\theta = K$  being the leading edge.

$L_6'(\phi)$ , the function tabulated, is part of  $L_6(\phi)$  for  $\alpha_0 = 7\frac{1}{2}$  deg, and is given directly in degrees.

For this value of  $\alpha_0$ ,

$$L_6(\phi) = L_6'(\phi) - 435.20465X(\phi).$$

For other values of  $\alpha_0$ ,

$$L_6(\phi) = 0.1316525 \cot \alpha_0, \quad L_6'(\phi) = 57.29578 \cot \alpha X(\phi).$$

First and second differences are given to enable interpolation to be performed, using the Besselian coefficients given in Table 6.

The reason for omitting the term containing  $X(\phi)$  from the tabulation is that it frequently cancels out with another term of  $\chi$ .

TABLE 4

$\theta$ deg	$L_6(\theta)$										
0	0										
1	0.0045	31	0.1480	61	0.3141	91	0.5435	121	0.9465	151	2.1016
2	0.0093	32	0.1530	62	0.3208	92	0.5531	122	0.9661	152	2.1831
3	0.0140	33	0.1579	63	0.3271	93	0.5625	123	0.9866	153	2.2711
4	0.0186	34	0.1633	64	0.3334	94	0.5731	124	1.0075	154	2.3663
5	0.0232	35	0.1683	65	0.3397	95	0.5831	125	1.0294	155	2.4695
6	0.0279	36	0.1733	66	0.3469	96	0.5933	126	1.0517	156	2.5822
7	0.0327	37	0.1783	67	0.3533	97	0.6083	127	1.0752	157	2.7054
8	0.0373	38	0.1838	68	0.3599	98	0.6150	128	1.0991	158	2.8411
9	0.0418	39	0.1891	69	0.3665	99	0.6256	129	1.1243	159	2.9912
10	0.0466	40	0.1941	70	0.3740	100	0.6368	130	1.1502	160	3.1587
11	0.0514	41	0.1993	71	0.3808	101	0.6483	131	1.1774	161	3.3468
12	0.0560	42	0.2049	72	0.3878	102	0.6599	132	1.2054	162	3.5600
13	0.0606	43	0.2101	73	0.3946	103	0.6720	133	1.2349	163	3.8049
14	0.0654	44	0.2155	74	0.4025	104	0.6841	134	1.2651	164	4.0902
15	0.0703	45	0.2207	75	0.4096	105	0.6967	135	1.2972	165	4.4310
16	0.0749	46	0.2267	76	0.4170	106	0.7094	136	1.3301	166	4.8583
17	0.0796	47	0.2321	77	0.4243	107	0.7226	137	1.3651	167	5.3989
18	0.0845	48	0.2376	78	0.4325	108	0.7358	138	1.4011	168	6.0547
19	0.0893	49	0.2430	79	0.4401	109	0.7497	139	1.4394	169	6.8134
20	0.0941	50	0.2489	80	0.4479	110	0.7637	140	1.4791	170	7.6508
21	0.0987	51	0.2546	81	0.4557	111	0.7782	141	1.5213	171	8.5308
22	0.1038	52	0.2602	82	0.4644	112	0.7928	142	1.5652	172	9.4058
23	0.1086	53	0.2658	83	0.4725	113	0.8083	143	1.6121	173	10.2142
24	0.1133	54	0.2720	84	0.4807	114	0.8236	144	1.6610	174	10.8784
25	0.1181	55	0.2777	85	0.4889	115	0.8399	145	1.7132	175	11.2992
26	0.1232	56	0.2836	86	0.4981	116	0.8562	146	1.7679	176	11.3454
27	0.1282	57	0.2894	87	0.5068	117	0.8733	147	1.8267	177	10.8336
28	0.1330	58	0.2959	88	0.5156	118	0.8907	148	1.8886	178	9.4744
29	0.1378	59	0.3020	89	0.5244	119	0.9087	149	1.9551	179	6.7014
30	0.1431	60	0.3081	90	0.5344	120	0.9272	150	2.0257	180	0

## Notes on Table 4

$L_6(\theta)$  as tabulated here is the complete conjugate of the leading-edge term for a symmetrical aerofoil. It is in degrees, and is given for  $\cot \alpha_0 = 9$ .

For other values of  $\alpha_0$ , the expression must be multiplied by  $\frac{1}{9} \cot \alpha_0$ .

TABLE 5

$\theta$ deg	$Q_6(\theta)$										
0	[124·18591]										
1	-49·03250	31	0·87204	61	0·23249	91	0·11690	121	0·07833	151	0·06324
2	-24·56713	32	0·81692	62	0·22567	92	0·11492	122	0·07756	152	0·06296
3	-11·12722	33	0·76707	63	0·21919	93	0·11301	123	0·07682	153	0·06269
4	-2·49626	34	0·72183	64	0·21302	94	0·11116	124	0·07610	154	0·06243
5	3·29487	35	0·68066	65	0·20714	95	0·10937	125	0·07540	155	0·06219
6	7·14583	36	0·64306	66	0·20153	96	0·10764	126	0·07472	156	0·06195
7	9·56006	37	0·60859	67	0·19617	97	0·10597	127	0·07407	157	0·06173
8	10·86246	38	0·57698	68	0·19105	98	0·10435	128	0·07343	158	0·06151
9	11·28767	39	0·54786	69	0·18615	99	0·10278	129	0·07281	159	0·06131
10	11·02183	40	0·52103	70	0·18147	100	0·10126	130	0·07221	160	0·06112
11	10·22498	41	0·49619	71	0·17700	101	0·09980	131	0·07163	161	0·06094
12	9·04494	42	0·47320	72	0·17272	102	0·09838	132	0·07107	162	0·06077
13	7·62871	43	0·45184	73	0·16862	103	0·09700	133	0·07053	163	0·06060
14	6·13779	44	0·43198	74	0·16468	104	0·09567	134	0·07000	164	0·06045
15	4·79781	45	0·41347	75	0·16090	105	0·09437	135	0·06949	165	0·06030
16	3·94527	46	0·39620	76	0·15728	106	0·09312	136	0·06899	166	0·06017
17	3·35155	47	0·38005	77	0·15380	107	0·09190	137	0·06851	167	0·06004
18	2·90055	48	0·36493	78	0·15046	108	0·09072	138	0·06804	168	0·05993
19	2·54405	49	0·35076	79	0·14726	109	0·08958	139	0·06759	169	0·05982
20	2·25485	50	0·33746	80	0·14418	110	0·08848	140	0·06715	170	0·05973
21	2·01573	51	0·32496	81	0·14122	111	0·08741	141	0·06673	171	0·05964
22	1·81505	52	0·31319	82	0·13836	112	0·08638	142	0·06632	172	0·05956
23	1·64454	53	0·30209	83	0·13561	113	0·08537	143	0·06593	173	0·05949
24	1·49817	54	0·29162	84	0·13297	114	0·08440	144	0·06555	174	0·05943
25	1·37144	55	0·28173	85	0·13042	115	0·08345	145	0·06518	175	0·05938
26	1·26083	56	0·27239	86	0·12796	116	0·08253	146	0·06482	176	0·05934
27	1·16365	57	0·26354	87	0·12558	117	0·08164	147	0·06448	177	0·05930
28	1·07774	58	0·25515	88	0·12330	118	0·08077	148	0·06415	178	0·05928
29	1·00139	59	0·24720	89	0·12109	119	0·07993	149	0·06383	179	0·05926
30	0·93321	60	0·23966	90	0·11896	120	0·07912	150	0·06353	180	0·05926

## Notes on Table 5

$Q_6(\theta)$  is the complete conjugate of the trailing-edge term, tabulated in degrees, for an upper surface velocity 2 less than on the lower surface, as in Appendix I, section 12. It is an even function of  $\theta$ .

The value at  $\theta = 0$  omits  $\frac{360}{\pi^2} \log \sin \frac{1}{2}\theta$ . This cancels out with another term of  $\chi$ .

TABLE 6  
*Coefficients of the Second Difference*

$n$	$-B$	$n$	$n$	$-B$	$n$	$n$	$-B$	$n$
0.000	0.000	1.000	0.090	0.021	0.910	0.210	0.042	0.790
0.002	0.001	0.998	0.095	0.022	0.905	0.217	0.043	0.783
0.006	0.001	0.994	0.100	0.023	0.900	0.224	0.043	0.776
0.010	0.002	0.990	0.105	0.024	0.895	0.231	0.044	0.769
0.014	0.003	0.986	0.110	0.025	0.890	0.239	0.045	0.761
0.018	0.004	0.982	0.115	0.026	0.885	0.247	0.047	0.753
0.022	0.005	0.978	0.120	0.027	0.880	0.255	0.048	0.745
0.026	0.006	0.974	0.125	0.028	0.875	0.263	0.049	0.737
0.030	0.007	0.970	0.131	0.029	0.869	0.271	0.050	0.729
0.035	0.008	0.965	0.136	0.030	0.864	0.280	0.051	0.720
0.039	0.009	0.961	0.142	0.031	0.858	0.290	0.052	0.710
0.043	0.010	0.957	0.147	0.032	0.853	0.300	0.053	0.700
0.048	0.011	0.952	0.153	0.033	0.847	0.310	0.054	0.690
0.052	0.012	0.948	0.159	0.034	0.841	0.321	0.055	0.679
0.057	0.013	0.943	0.165	0.035	0.835	0.332	0.056	0.668
0.061	0.014	0.939	0.171	0.036	0.829	0.345	0.057	0.655
0.066	0.015	0.934	0.177	0.037	0.823	0.358	0.058	0.642
0.071	0.016	0.929	0.183	0.038	0.817	0.373	0.059	0.627
0.075	0.017	0.925	0.190	0.039	0.810	0.390	0.060	0.610
0.080	0.018	0.920	0.196	0.040	0.804	0.410	0.061	0.590
0.085	0.019	0.915	0.203	0.041	0.797	0.436	0.062	0.564
0.090	0.020	0.910	0.210	0.041	0.790	0.500	0.062	0.500

$B = n(n - 1)/4$  and is always negative. In critical cases in the table ascend.

#### *Notes on Table 6*

Let successive values of a function, and its first and second differences be as follows:—

$$\begin{array}{ccccc}
 f_{-1} & & a & & \\
 & & f_0 & & d \\
 & & b & & \\
 f_1 & & c & & e \\
 & & f_2 & &
 \end{array}$$

Then to find the value  $f_n$  at a fraction  $n$  of the interval from  $f_0$  to  $f_1$ , Bessel's formula gives

$$\begin{aligned}
 f_n &= f_0 + nb + \frac{n(n-1)}{4} (d + e) \\
 &= f_0 + nb + B(d + e).
 \end{aligned}$$

The values of  $B$  are given here as a critical table. Choose the value of  $B$  corresponding to the interval in which the required value of  $n$  lies.

TABLE 7

$\theta$ deg	$\chi$	$(e^l/q_0)$ $\sin \theta \cos \chi$	$(e^l/q_0)$ $\sin \theta \sin \chi$	$x$	$y$	$X$	$Y$	$q_0$	$q_1$
360	$180^\circ + 3^\circ 54 \cdot 8'$	0	0	0	0	1.00000	0	0.72917	0.70432
355	$+ 4^\circ 56 \cdot 8'$	-0.13962	-0.01208	0.216	-0.016	0.99705	-0.00071	0.79449	0.75844
350	$+ 4^\circ 14 \cdot 0'$	-0.26017	-0.01926	-0.819	-0.068	0.98881	-0.00279	0.85036	0.80213
345	$+ 2^\circ 50 \cdot 2'$	-0.37550	-0.01861	-1.772	-0.123	0.97574	-0.00571	0.87949	0.81956
340	$+ 2^\circ 39 \cdot 9'$	-0.48855	-0.02274	-3.069	-0.184	0.95792	-0.00949	0.89340	0.82219
335	$+ 3^\circ 1 \cdot 3'$	-0.59155	-0.03123	-4.693	-0.264	0.93562	-0.01427	0.91143	0.82808
330	$+ 3^\circ 31 \cdot 3'$	-0.68286	-0.04202	-6.607	-0.374	0.90937	-0.02012	0.93367	0.83711
325	$+ 4^\circ 0 \cdot 7'$	-0.76124	-0.05339	-8.777	-0.517	0.87964	-0.02701	0.96023	0.84915
320	$+ 4^\circ 23 \cdot 9'$	-0.82600	-0.06353	-11.161	-0.693	0.84703	-0.03484	0.99124	0.86409
310	$+ 4^\circ 33 \cdot 5'$	-0.91421	-0.07289	-16.409	-1.112	0.77532	-0.05251	1.06711	0.90196
300	$+ 3^\circ 22 \cdot 4'$	-0.95024	-0.05601	-22.027	-1.515	0.69844	-0.07080	1.16230	0.94901
290	$- 0^\circ 54 \cdot 8'$	-0.93957	+0.01498	-27.719	-1.675	0.61999	-0.08588	1.27754	1.00248
280	$- 5^\circ 59 \cdot 1'$	-0.97994	0.10268	-33.492	-1.298	0.53921	-0.09372	1.27754	0.95956
270	$- 9^\circ 10 \cdot 5'$	-0.98721	0.15945	-39.408	-0.505	0.45550	-0.09612	1.27754	0.90336
260	$- 11^\circ 58 \cdot 4'$	-0.96338	0.20430	-45.275	+0.591	0.37179	-0.09422	1.27754	0.83995
250	$- 14^\circ 44 \cdot 3'$	-0.90878	0.23906	-50.907	1.927	0.29079	-0.08846	1.27754	0.76179
240	$- 17^\circ 43 \cdot 7'$	-0.82490	0.26371	-56.122	3.440	0.21516	-0.07930	1.27754	0.66130
230	$- 21^\circ 15 \cdot 7'$	-0.71390	0.27779	-60.752	5.070	0.14737	-0.06720	1.27754	0.52492
220	$- 25^\circ 52 \cdot 6'$	-0.57834	0.28054	-64.640	6.751	0.08973	-0.05272	1.27754	0.32555
210	$- 32^\circ 47 \cdot 6'$	-0.42031	0.27081	-67.647	8.411	0.04434	-0.03654	1.27754	0
207 $\frac{1}{2}$	$- 35^\circ 11 \cdot 8'$	-0.37733	0.26615	-68.245	8.814	0.03515	-0.03231	1.27754	0.11725
205	$- 38^\circ 2 \cdot 7'$	-0.33282	0.26045	-68.778	9.209	0.02688	-0.02805	1.27754	0.25746
202 $\frac{1}{2}$	$- 41^\circ 30 \cdot 4'$	-0.28658	0.25361	-69.243	9.595	0.01957	-0.02376	1.27754	0.42829
200	$- 45^\circ 51 \cdot 1'$	-0.23822	0.24541	-69.637	9.969	0.01327	-0.01947	1.27754	0.64121
197 $\frac{1}{2}$	$- 51^\circ 33 \cdot 8'$	-0.18693	0.23554	-69.956	10.330	0.00803	-0.01519	1.27754	0.91427
195	$- 59^\circ 41 \cdot 2'$	-0.13063	0.22343	-70.195	10.675	0.00394	-0.01096	1.27754	1.27754
192 $\frac{1}{2}$	$180^\circ - 73^\circ 25 \cdot 9'$	-0.06191	0.20810	-70.342	10.999	0.00118	-0.00680	1.27354	1.77956
190	$85^\circ 25 \cdot 3'$	+0.01856	0.23174	-70.368	11.329	0.00007	-0.00229	0.95422	1.90117
187 $\frac{1}{2}$	$74^\circ 43 \cdot 7'$	0.06891	0.25239	-70.301	11.693	0.00017	+0.00290	0.63736	1.90117
185	$66^\circ 54 \cdot 0'$	0.11402	0.26731	-70.164	12.083	0.00119	0.00861	0.38315	1.90117
182 $\frac{1}{2}$	$60^\circ 42 \cdot 8'$	0.15623	0.27854	-60.961	12.493	0.00307	0.01475	0.17449	1.90117
180	$55^\circ 36 \cdot 4'$	0.19648	0.28703	-69.696	12.918	0.00578	0.02123	0	1.90117
170	$41^\circ 6 \cdot 1'$	0.34506	0.30103	-68.062	14.696	0.02438	0.04954	0.48447	1.90117
160	$31^\circ 24 \cdot 7'$	0.47737	0.29152	-65.588	16.483	0.05460	0.07988	0.78117	1.90117
150	$23^\circ 59 \cdot 9'$	0.59297	0.26399	-62.367	18.158	0.09540	0.11036	0.98412	1.90117
140	$17^\circ 48 \cdot 9'$	0.68964	0.22164	-58.510	19.622	0.14550	0.13935	1.13366	1.90117
130	$12^\circ 19 \cdot 3'$	0.76490	0.16708	-54.134	20.793	0.20344	0.16546	1.24998	1.90117
120	$7^\circ 10 \cdot 4'$	0.81656	0.10277	-49.378	21.607	0.26745	0.18749	1.34433	1.90117
110	$2^\circ 6 \cdot 1'$	0.84277	0.03093	-44.387	22.011	0.33564	0.20437	1.42351	1.90117
100	$- 3^\circ 9 \cdot 1'$	0.84206	-0.04637	-39.319	21.967	0.40591	0.21523	1.49184	1.90117
90	$- 8^\circ 54 \cdot 7'$	0.81306	-0.12749	-34.339	21.447	0.47604	0.21929	1.55230	1.90117
80	$- 15^\circ 42 \cdot 5'$	0.75369	-0.21197	-29.623	20.431	0.54363	0.21589	1.60695	1.90117
70	$- 24^\circ 39 \cdot 3'$	0.65834	-0.30217	-25.366	18.892	0.60606	0.20421	1.65729	1.90117
60	$- 39^\circ 14 \cdot 6'$	0.50269	-0.41062	-21.844	16.768	0.65963	0.18276	1.70455	1.90117
57 $\frac{1}{2}$	$- 45^\circ 11 \cdot 6'$	0.44249	-0.44549	-21.135	16.127	0.67089	0.17549	1.71599	1.90117
55	$- 53^\circ 32 \cdot 7'$	0.35999	-0.48730	-20.528	15.428	0.68088	0.16719	1.72732	1.90117
52 $\frac{1}{2}$	$- 67^\circ 46 \cdot 8'$	0.22046	-0.53969	-20.083	14.659	0.68878	0.15755	1.73853	1.90117
50	$- \infty$	—	—	-20.040	13.860	0.69109	0.14684	1.74963	1.90117
47 $\frac{1}{2}$	$- 67^\circ 44 \cdot 4'$	-0.62444	1.52558	-19.923	11.477	0.69819	0.11385	0.57139	0.61700
45	$- 53^\circ 27 \cdot 6'$	-0.93547	1.26237	-18.721	9.394	0.7954	0.08773	0.57495	0.61700
42 $\frac{1}{2}$	$- 45^\circ 3 \cdot 7'$	-1.05386	1.05613	-17.212	7.661	0.74436	0.06715	0.57849	0.61700
40	$- 39^\circ 3 \cdot 3'$	-1.09568	0.88901	-15.598	6.206	0.77000	0.05065	0.58200	0.61700
35	$- 30^\circ 26 \cdot 5'$	-1.07258	0.63033	-12.322	3.946	0.82047	0.02677	0.58900	0.61700
30	$- 24^\circ 6 \cdot 2'$	-0.97836	0.43771	-9.234	2.358	0.86681	0.01176	0.59597	0.61700
25	$- 18^\circ 54 \cdot 0'$	-0.84718	0.29005	-6.489	1.275	0.90727	0.00298	0.60295	0.61700
20	$- 14^\circ 15 \cdot 7'$	-0.69429	0.17648	-4.172	0.584	0.94091	-0.00135	0.60994	0.61700
15	$- 9^\circ 45 \cdot 1'$	-0.52816	0.09077	-2.336	0.188	0.96723	-0.00268	0.61700	0.61700
10	$- 4^\circ 15 \cdot 1'$	-0.35063	0.02607	-1.015	0.018	0.98591	-0.00205	0.63096	0.62375
5	$+ 0^\circ 41 \cdot 9'$	-0.16599	-0.00202	-0.240	-0.005	0.99669	-0.00061	0.67074	0.65546
0	$3^\circ 54 \cdot 8'$	0	0	0	0	1.00000	0	0.72917	0.70432

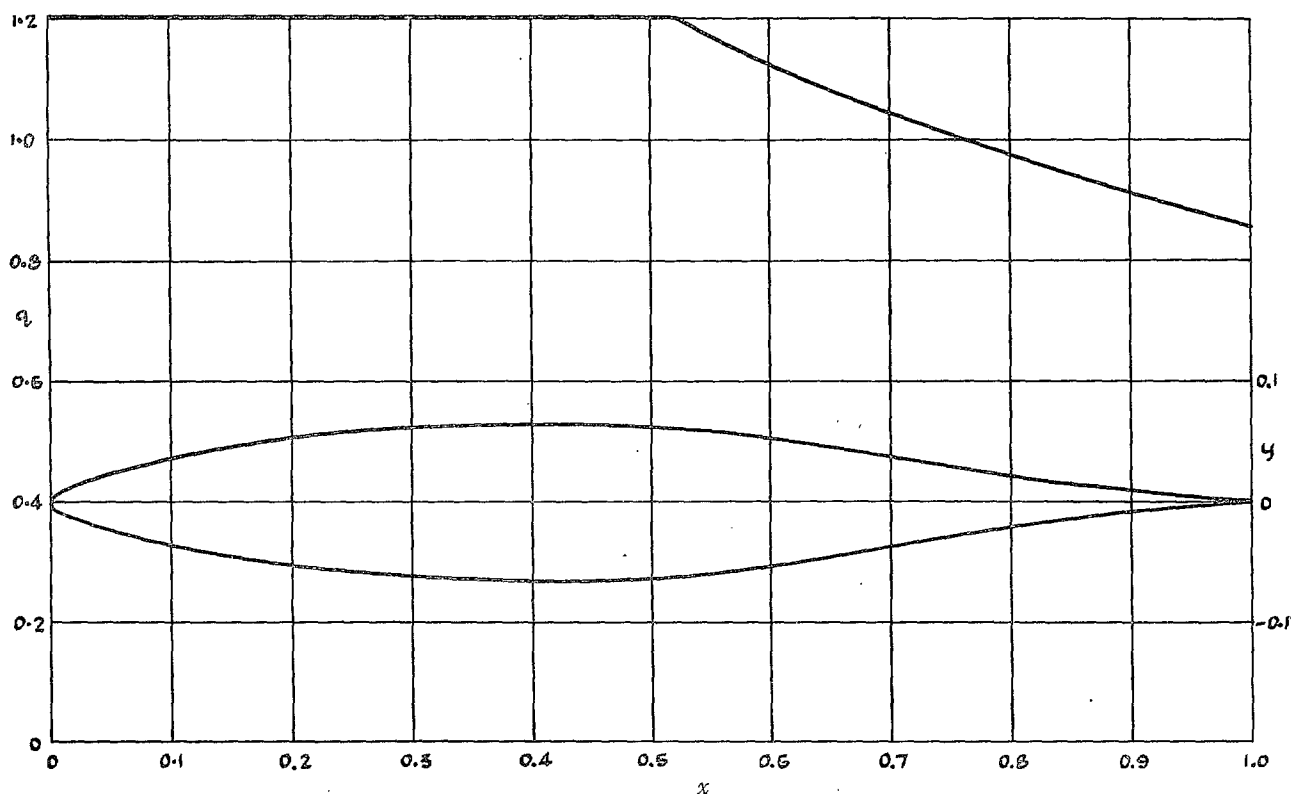


FIG. 1. Laminar flow aerofoil 13.0 per cent thick.

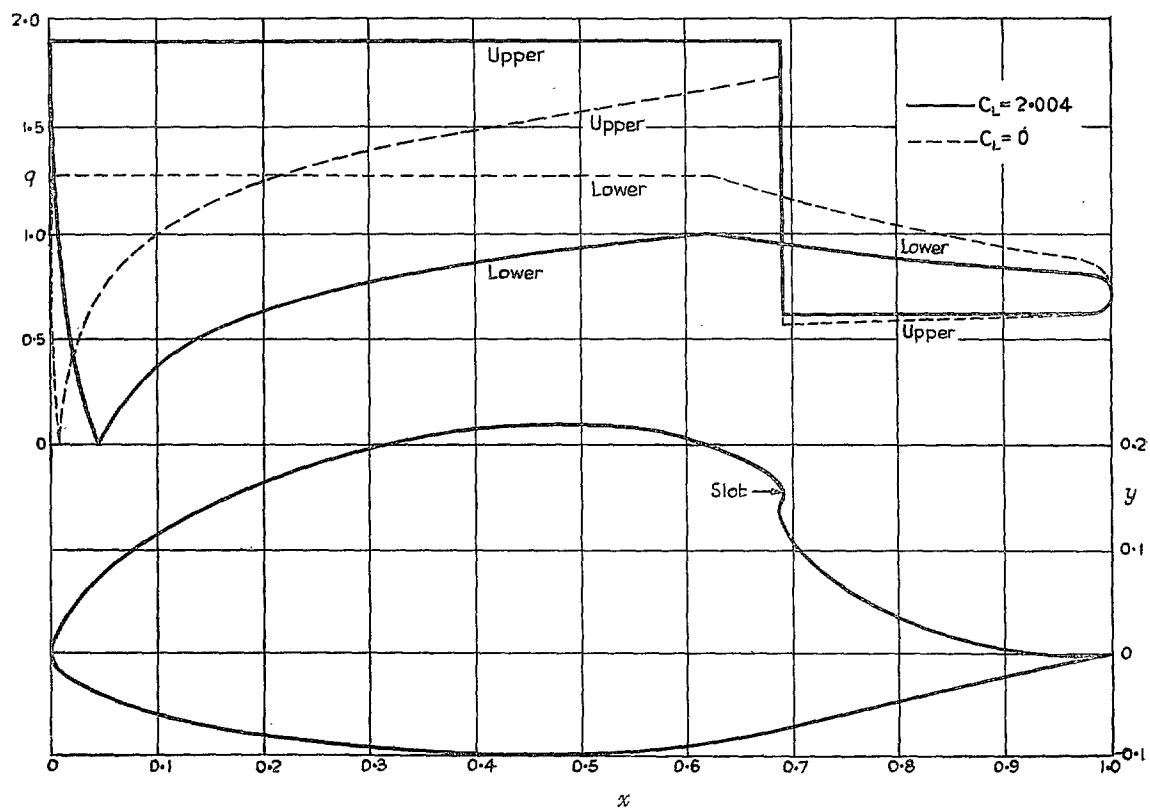


FIG. 2. Suction aerofoil with a single slot 31.5 per cent thick.

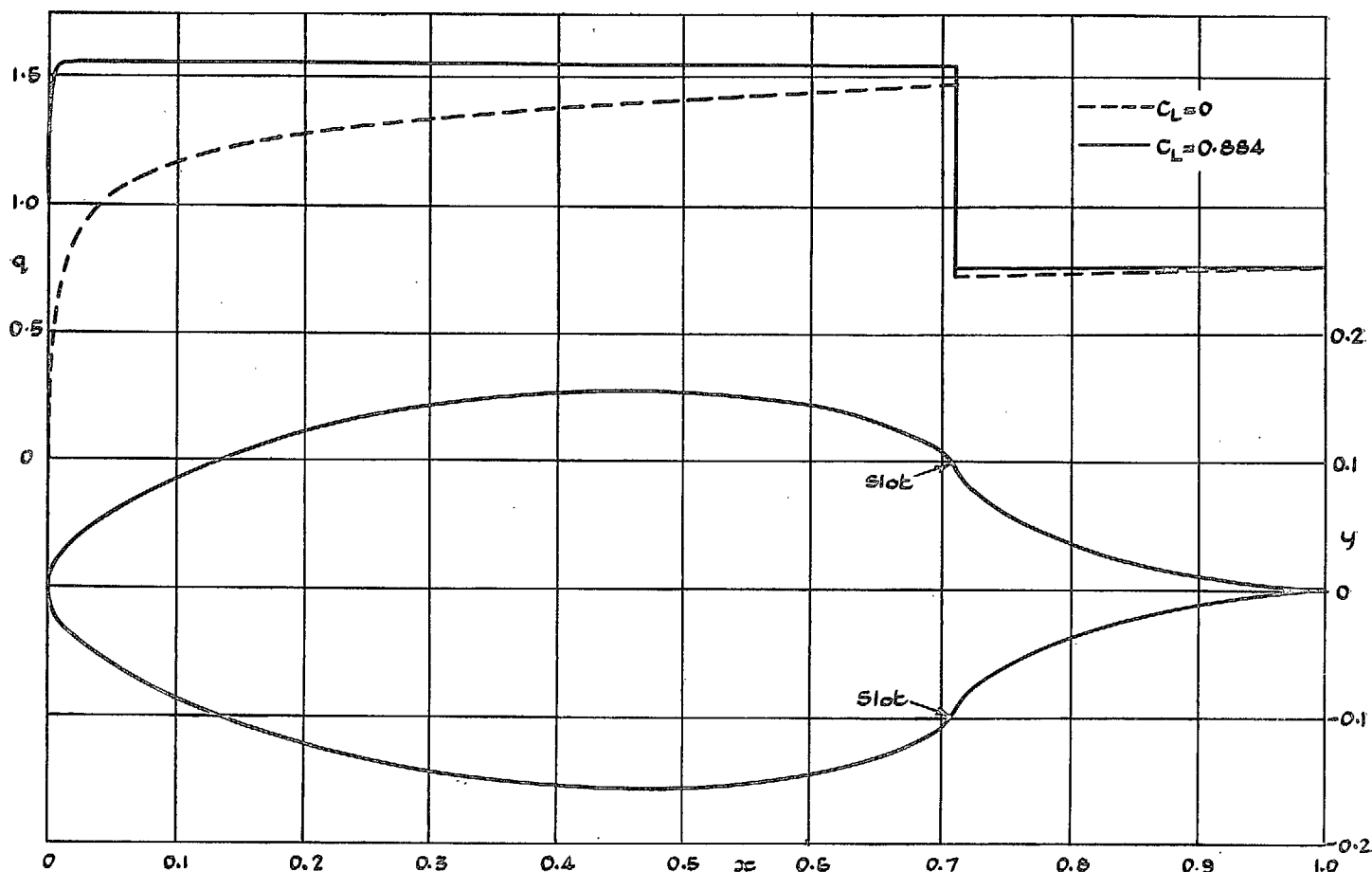


FIG. 3. Symmetrical suction aerofoil 31·2 per cent thick.

## Publications of the Aeronautical Research Council

### ANNUAL TECHNICAL REPORTS OF THE AERONAUTICAL RESEARCH COUNCIL (BOUND VOLUMES)—

- 1936 Vol. I. Aerodynamics General, Performance, Airscrews, Flutter and Spinning.  
40s. (41s. 1d.)  
Vol. II. Stability and Control, Structures, Seaplanes, Engines, etc. 50s. (51s. 1d.)
- 1937 Vol. I. Aerodynamics General, Performance, Airscrews, Flutter and Spinning.  
40s. (41s. 1d.)  
Vol. II. Stability and Control, Structures, Seaplanes, Engines, etc. 60s. (61s. 1d.)
- 1938 Vol. I. Aerodynamics General, Performance, Airscrews. 50s. (51s. 1d.)  
Vol. II. Stability and Control, Flutter, Structures, Seaplanes, Wind Tunnels,  
Materials. 30s. (31s. 1d.)
- 1939 Vol. I. Aerodynamics General, Performance, Airscrews, Engines. 50s. (51s. 1d.)  
Vol. II. Stability and Control, Flutter and Vibration, Instruments, Structures,  
Seaplanes, etc. 63s. (64s. 2d.)
- 1940 Aero and Hydrodynamics, Aerofoils, Airscrews, Engines, Flutter, Icing, Stability  
and Control, Structures, and a miscellaneous section. 50s. (51s. 1d.)
- 1941 Aero and Hydrodynamics, Aerofoils, Airscrews, Engines, Flutter, Stability and  
Control, Structures. 63s. (64s. 2d.)
- 1942 Vol. I. Aero and Hydrodynamics, Aerofoils, Airscrews, Engines. 75s. (76s. 3d.)  
Vol. II. Noise, Parachutes, Stability and Control, Structures, Vibration, Wind  
Tunnels. 47s. 6d. (48s. 7d.)
- 1943 Vol. I. Aerodynamics, Aerofoils, Airscrews. 80s. (81s. 4d.)  
Vol. II. Engines, Flutter, Materials, Parachutes, Performance, Stability and Control,  
Structures. 90s. (91s. 6d.)
- 1944 Vol. I. Aero and Hydrodynamics, Aerofoils, Aircraft, Airscrews, Controls. 84s.  
(85s. 8d.)  
Vol. II. Flutter and Vibration, Materials, Miscellaneous, Navigation, Parachutes,  
Performance, Plates and Panels, Stability, Structures, Test Equipment,  
Wind Tunnels. 84s. (85s. 8d.)

### ANNUAL REPORTS OF THE AERONAUTICAL RESEARCH COUNCIL—

1933-34	1s. 6d. (1s. 8d.)	1937	2s. (2s. 2d.)
1934-35	1s. 6d. (1s. 8d.)	1938	1s. 6d. (1s. 8d.)
April 1, 1935 to Dec. 31, 1936.	4s. (4s. 4d.)	1939-48	3s. (3s. 2d.)

### INDEX TO ALL REPORTS AND MEMORANDA PUBLISHED IN THE ANNUAL TECHNICAL REPORTS, AND SEPARATELY—

April, 1950 . . . . . R. & M. No. 2600. 2s. 6d. (2s. 7½d.)

### AUTHOR INDEX TO ALL REPORTS AND MEMORANDA OF THE AERONAUTICAL RESEARCH COUNCIL—

1909-1949 . . . . . R. & M. No. 2570. 15s. (15s. 3d.)

### INDEXES TO THE TECHNICAL REPORTS OF THE AERONAUTICAL RESEARCH COUNCIL—

December 1, 1936 — June 30, 1939.	R. & M. No. 1850.	1s. 3d. (1s. 4½d.)
July 1, 1939 — June 30, 1945.	R. & M. No. 1950.	1s. (1s. 1½d.)
July 1, 1945 — June 30, 1946.	R. & M. No. 2050.	1s. (1s. 1½d.)
July 1, 1946 — December 31, 1946.	R. & M. No. 2150.	1s. 3d. (1s. 4½d.)
January 1, 1947 — June 30, 1947. July, 1951.	R. & M. No. 2250. R. & M. No. 2350.	1s. 3d. (1s. 4½d.) 1s. 9d. (1s. 10½d.)

*Prices in brackets include postage.*

Obtainable from

HER MAJESTY'S STATIONERY OFFICE

York House, Kingsway, London, W.C.2; 423 Oxford Street, London, W.1 (Post Orders: P.O. Box 569, London, S.E.1);  
13a Castle Street, Edinburgh 2; 39 King Street, Manchester 2; 2 Edmund Street, Birmingham 3; 1 St. Andrew's  
Crescent, Cardiff; Tower Lane, Bristol 1; 80 Chichester Street, Belfast, or through any bookseller.